



Modelling the production of biodiesel from non-edible oils (*Jatropha curcas* oil and Tobacco seed oil (TSO): A kinetic study

Prepared by

Feziwe Mthembu

Thesis submitted in partial fulfilment of the requirements for the degree of **Master of Science in Engineering** at the School of Chemical and Metallurgical Engineering, Faculty of Engineering and the Built Environment, University of the Witwatersrand

Supervisor: Dr D. Nkazi

Johannesburg, South Africa

October, 2017

Plagiarism declaration



University of the Witwatersrand, Johannesburg, South Africa
Faculty of Engineering and the Built Environment
School of Chemical and Metallurgical Engineering

Plagiarism Declaration for Postgraduate Research

I FEZIWE CELILE MTHEMBU
(Student number: 471506) am a student registered for MSc ENG
in the year 2017. I hereby declare the following:

- I am aware that plagiarism (the use of someone else's work without their permission and/or without acknowledging the original source) is wrong.
- I confirm that the work submitted for assessment for the above course is my own unaided work except where I have explicitly indicated otherwise.
- I have followed the required conventions in referencing the thoughts and ideas of others.
- I understand that the University of the Witwatersrand may take disciplinary action against me if there is a belief that this is not my own unaided work or that I have failed to acknowledge the source of the ideas or words in my writing.

Student Signature:  Date: 25 October 2017

Acknowledgements

I would like to acknowledge the Oil and Gas Engineering research group of the School of Chemical and Metallurgical Engineering at the University of the Witwatersrand for the opportunity given to me to conduct this research project and for their support during my research journey and to CHIETA South Africa for funding my study.

I would also like to extend my sincerest gratitude to my supervisor, Dr Diakanua Nkazi for his endless support and mentorship during the course of this study. I appreciate the assistance of the support staff of the School of Chemical and Metallurgical engineering, during the course of this project which includes but not limited to Mr Bruce Mothibedi (lab manager) and postgraduate officer, Ms Notokozo Dube. I also acknowledge Mr Tasekela Ng'ambi (BSc Chem Eng. University of Cape Town alumni, Sasol ltd.) for his contributions in the simulations section. I also acknowledge and appreciate the work used in this study as reference for the validation of the proposed model and the brilliant researchers who paved way for this to happen. Last but not least, I am profoundly grateful for the support of my family, friends, as well as the 2016 Petroleum engineering students.

Abstract

The significant increase in the primary energy demand and the effort to reduce harmful emissions related to the greenhouse gases enhanced the search for alternative energy. Production and modelling processes of biofuel from non-edible oil sources assist in the process development of an environmentally friendly fuel such as biodiesel. This work focused on the kinetic modelling of biodiesel synthesised from non-edible oils. Two types of non-edible oils (Jatropha curcas seed oil and Tobacco seed oil) were used in this study including the development of the kinetic behaviour of the transesterification reaction. A linear polynomial model was generated from experimental data found in literature in order to study the influence of operating parameters during biodiesel production. It was found that the temperature improves the yield of biodiesel; this is attributed to the fact that temperature affects the reaction rate constants; and the higher the reaction rate, the lower the activation energy required for a reaction to occur. The optimum conditions for the transesterification of Jatropha curcas seed oil are a temperature of 55 °C, methanol to oil ratio of 6:1, catalyst concentration of 1.2% KOH (by volume of oil), and agitation speed range of 0-250 rpm. Results from both the homogeneous and heterogeneous reactions of Jatropha curcas oil and tobacco seed oil were used to verify the theoretical kinetic and empirical models. It was found that both models describe the kinetic behaviour of transesterification with minor deviations in the estimated parameters. However, the use of empirical model in determining the reaction order, as opposed to the theoretical assumption, gave a second order with respect to oil triglycerides at a temperature of 60 °C. The theoretical kinetic model gave a first order with respect to oil triglycerides. In this case, the activation energy was found to be 71.83 kJ/mol and pre-exponential factor was found to be 2.48×10^{10} . More investigation should be done to describe the kinetic behaviour of biodiesel production from non-edible oil in order to confirm the correct reaction order and why there is change in reaction order when the temperature increases above 60°C.

Contents

Plagiarism declaration.....	ii
Acknowledgements.....	iii
Abstract.....	iv
List of Figures.....	vii
List of Tables.....	ix
List of Symbols, abbreviations and Nomenclature.....	x
1. Introduction.....	1
1.1 Motivation and Background.....	1
1.2 Research Objectives.....	3
1.3 Research Questions.....	3
1.4 Scope of Study.....	3
1.5 Expected Outcome and Benefits.....	4
2. Literature Review.....	5
2.1 Biodiesel Chemical Building Blocks.....	5
2.2 Feedstock for Biodiesel Production.....	7
2.2.1 Common non-edible Oils.....	7
2.3 Principles of Biodiesel Production.....	8
2.4 Chemical Reactions involved.....	10
2.5 Transesterification thermodynamics and reaction kinetics.....	14
2.6 Kinetic Models.....	17
2.6.1 Freedman's Kinetic Model.....	17
2.6.2 Komers' Kinetic Model.....	19
2.6.3 Other Models.....	21
2.7 Parameters that influence the transesterification reaction.....	21
2.8 Optimization of non-edible oil transesterification.....	24
3. Methodology.....	25
3.1. Derivation of theoretical kinetic model.....	26
3.2. Kinetic Parameters.....	28
4. Results and Discussion.....	29
4.1 Kinetic models and Response surface methodology.....	29
4.1.1 Response Surface Methodology.....	29
4.1.2 Kinetic model from literature.....	33

4.1.3 Empirical model.....	38
4.1.4 Model validation	49
(a) Tobacco Seed oil.....	50
(b) Jatropha Curcas oil.....	53
5. Conclusion	55
6. Recommendations.....	56
7. References.....	57
Appendices.....	63
Appendix A: Komers Model Derivation.....	64
Appendix B: Experimental Data Sheets.....	70
Appendix C: Simulation Codes.....	75

List of Figures

Figure 2-1: Idealized fatty acid molecular structure (Turner, 2005).....	5
Figure 2-2: Molecular structure of soap (Turner, 2005)	5
Figure 2-3: Molecular structure of glycerol (Turner, 2005)	6
Figure 2-4: Molecular structures of methanol, ethanol, and 1-propanol (Turner, 2005)	6
Figure 2-5: Molecular structure of methyl ester (Turner, 2005).....	6
Figure 4-6: Experimental concentration-time data <i>Jatropha curcas</i> oil transesterification at T=50°C (Mu'azu, <i>et al.</i> , 2015)	35
Figure 4-7: Scilab Simulated model at T=50°C.....	35
Figure 4-8: Experimental concentration-time data <i>Jatropha curcas</i> oil transesterification at T=55°C (Mu'azu, <i>et al.</i> , 2015)	36
Figure 4-9: Scilab simulated model at T=55°C	36
Figure 4-10: Determining activation energy and pre-exponential factor	38
Figure 4-11: Variation of TG with time assuming first order kinetics at T=45°C, k=0.041/L	41
Figure 4-12: Verification of first order kinetics at T=45°C	41
Figure 4-13: Variation of TG with time assuming first order kinetics at T=50°C, k=0.055/L	42
Figure 4-14: Verification of first order kinetics at T=50°C	42
Figure 4-15: Variation of TG with time assuming first order kinetics at T=55°C, k=0.094/L	43
Figure 4-16: Verification of first order kinetics at T=55°C	44
Figure 4-17: Variation of TG with time assuming second order kinetics at T=45°C, k=0.010045 L/mol/min	45
Figure 4-18: Verification of second order kinetics, T=45°C	45
Figure 4-19: Variation of TG with time assuming second order kinetics at T=50°C, k=0.0125L/mol/min	46
Figure 4-20: Verification of second order kinetics at T=50°C	46
Figure 4-21: Variation of TG with time assuming second order kinetics at T=55°C, k=0.033 L/mol/min	47
Figure 4-22: Verification of second order kinetics at T=55°C	47
Figure 4-23: Activation energy and pre-exponential factor (First order kinetics)	48
Figure 4-24: Activation energy and pre-exponential factor	49
Figure 4-25: Experimental concentration-time data, T=60°C (Veljkovic', <i>et al.</i> , 2006).....	50
Figure 4-26: Simulated results of the variation of TG with time assuming first order kinetics at T=60°C, k=0.23/L.....	51

Figure 4-27: verification of first order kinetics, $T=60^{\circ}\text{C}$	51
Figure 4-28: Simulated results for the variation of TG with time assuming second order kinetics at $T=60^{\circ}\text{C}$, $k=0.0138\text{L/mol/min}$	52
Figure 4-29: Verification of second order kinetics, $T=60^{\circ}\text{C}$	52
Figure 4-30: Verification of first order kinetics at $T=50^{\circ}\text{C}$	53
Figure 4-31: Verification of first order kinetics at $T=60^{\circ}\text{C}$	53
Figure 4-32: Verification of second order kinetics at $T=50^{\circ}\text{C}$	54
Figure 4-33: Verification of second order kinetics at $T=60^{\circ}\text{C}$	54

List of Tables

Table 2-1: Two-step homogeneously catalysed process for different non-edible oils.....	13
Table 2-2: Physical Properties of Diesel and Biodiesel Fuels	15
Table 2-3: Summary of different kinetic models (Liu, 2013).....	21
Table 4-1: 2 ³ Design summaries	29
Table 4-5: Verification of order of reaction.....	39

List of Symbols, abbreviations and Nomenclature

FAME	Fatty acids methyl esters
FFA	Free Fatty Acid(s)
MAG/MG	Monoacylglycerol/ Monoglyceride
DAG/DG	Diacylglycerol/ Diglyceride
TAG/TG	Triacylglycerol/Triglyceride
E	Alkyl Ester(s)
A	Soap
W	Water
SVO	Straight Vegetable Oil
WVO	Waste Vegetable Oil
LMA	Law of Mass Action
mg/l	Milligrams per litre
% w/w	Weight percentage per weight

CHAPTER 1

1. Introduction

1.1 Motivation and Background

The ever increasing global population exerts a rising demand on energy resources, and with the current rate of energy consumption and cost, particularly of petroleum based fuels, there remain a threat of the depletion of oil reserves where supply no longer meets demand (Janaun & Ellis, 2010).

Biofuels provide a sustainable solution to the current energy demands, depleting fuel reserves, and environmental issues that accompany the use of fossil fuels such as coal, petroleum oil and gas. Petroleum based fuels have proven to have negative environmental impacts over time, as they result in high greenhouse gas emissions thus causing global warming (Ma & Hanna, 1999).

In an attempt to reduce greenhouse gases, particularly carbon dioxide, vast research has been conducted on the viability of biofuels and great interest has been paid particularly to vegetable-based fuels such as biodiesel. Biodiesel provides an ecologically friendly substitution to mineral diesel as it is biodegradable, renewable, and has low sulphur contents (Ma & Hanna, 1999). Biodiesel is 100% vegetable-based and does not contain petroleum diesel; it is a naturally oxygenated fuel comprising of 10% of oxygen, and because of the plant's innate ability to absorb the sun's energy through photosynthesis whilst effectively capturing carbon dioxide from the atmosphere as their primary food source, it results in the net CO₂ emission of virtually zero (Janaun & Ellis, 2010).

The production of biodiesel as a substitution for petroleum diesel stands to benefit the communities by encouraging job opportunities, developing the economy of rural areas, reducing dependency on petroleum imports, and increasing the security of energy supply (Bankovic-Ilic *et al.*, 2012).

Currently, global biodiesel production is heavily dependent (over 95%) on edible oils as the main feedstock (Gui *et al.*, 2008). The use of edible oils for biodiesel production poses many problems since it causes an imbalance to the market demand and food supply. Attention should therefore be shifted to non-edible oil sources, which due to the presence of toxic

compounds, are not suitable for human consumption and could grow in waste lands (Shika & Rita, 2012).

Globally, there are abundant non-edible oil plants that are present in nature which can provide a much more cost effective solution than the edible oil plants. Jatropha oil, Neem oil, Mahua oil, Castor oil, Cotton seed oil, Karanja oil, Tobacco oil, and Soapnut oil are amongst the non-edible oil sources that are easily available in developing countries (Bankovic-Ilic *et al.*, 2012).

Most developing countries, particularly African countries, face the challenge of poverty and shortage of food supply therefore utilising edible oils for biofuel production will be an impractical option. With biodiesel produced from non-edible oils, the transition to renewable energy in African countries is feasible. Recently, farmers in Limpopo province, South Africa, cultivated nicotine-free, high energy solaris tobacco plants that were used as non-edible oil feedstock blended with conventional fuel by the first commercial planes in Africa. These Boeing jets operated by South African Airways (SAA) carried 300 passengers between Johannesburg and Cape Town on the 15th of July 2016 (ESI Africa, 2016). A mixture of 30% biofuel and 70% conventional fossil fuel was used for the flights. SAA aims to have 50% of its fleet operating on biofuel by 2023, which could reach a capacity of 500 million litres per year (ESI Africa, 2016).

The production of second generation biofuels from non-edible oils needs the extensive understanding of the parameters that influence production in order to optimize and improve biodiesel yield and quality. Reaction kinetics plays an important role in biodiesel synthesis, and although there is a wealth of knowledge in literature on the production of biodiesel from non-edible oils, the reaction kinetics remain controversial (Bankovic-Ilic *et al.*, 2012).

This research project focuses on the modelling of biodiesel production from low free fatty acid (FFA) of non-edible oils by studying the influence of operating parameters and reaction kinetics during biodiesel synthesis. The aim is to fit a general predictive kinetic model for jatropha curcas oil and tobacco seed oil and to explore whether there is a general model that describes the kinetic behaviour of different non-edible oils.

1.2 Research Objectives

The aim of this research is to establish a predictive kinetic model for transesterification of non-edible oils (*Jatropha curcas* seed oil and Tobacco seed oil) for biodiesel synthesis. This is achieved by the following objectives;

- Deriving an empirical model from the concentration-time data found in literature and attempt to establish the order of the reactions and rate constants;
- Fitting a theoretical model found in literature by assuming a set of reaction mechanisms, and then assuming the rate of reaction based on the law of mass action (LMA).
- Fitting the experimental data on the kinetic models and minimize error by means of least square analysis.
- Comparing the theoretical and empirical models to ascertain what model is more predictive.
- Performing a study of influencing parameters on biodiesel production using surface response methodology (RSM).

1.3 Research Questions

- a) Does the kinetic behaviour of different non-edible oils vary and to what degree?
- b) Can there be a global kinetic model that best fits data with least errors and variations for the majority of non-edible oil feedstock?
- c) To what degree would the said kinetic model fit the data and how can the models be optimised to describe the general behaviour of biodiesel production from non-edible oils?
- d) What parameters have more influence on the biodiesel yield, and how can they be optimised for higher yields at lower costs and low energy consumption?

1.4 Scope of Study

This research applies to the transesterification of non-edible oils, mainly *Jatropha curcas* oil and Tobacco seed oil with low FFA content (<3%) under heterogeneous and homogenous base catalysis respectively, and studies the effect of kinetics on biodiesel yield. The model to be derived does not cover the non-kinetic effects such as process economics, feedstock

quantity, reactor material etc., and does not take into account the effect of competing reactions since the FFA content of the oil is low.

1.5 Expected Outcome and Benefits

This project is an attempt to derive a general kinetic model that allows the evaluation of transesterification of two non-edible oils (*Jatropha curcas* oil and Tobacco seed oil) for biodiesel synthesis at different conditions. This research will contribute to a better understanding of reaction kinetics in biodiesel production and provide more knowledge of what parameters are most important when producing biodiesel. The derived model will be useful in predicting the extent of reaction and determining the optimum conditions for maximum biodiesel yield.

CHAPTER 2

2. Literature Review

2.1 Biodiesel Chemical Building Blocks

Chemically, biodiesel is a fatty acid alkyl ester typically produced from the reaction of vegetable oil with an alcohol in the presence of a catalyst. In order to understand how biodiesel is produced from non-edible oil, one has to first understand the chemical building foundations of biodiesel making.

Fatty Acids

Fatty acids are carboxylic acids that are present in both biodiesel and the non-edible vegetable oils. The idealised molecular structure of a fatty acid is shown below in Figure 2-1. The term free fatty acids (FFA) refers to fatty acids that are not bound to other molecules (Turner, 2005).

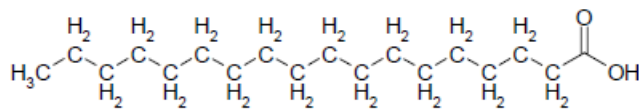


Figure 2-1: Idealized fatty acid molecular structure (Turner, 2005)

The major drawback with oils that contain high FFA content is that it leads to formation of soap under base catalysis as the FFA tends to react with the base catalyst. Figure 2-2 is a molecular structure of soap.

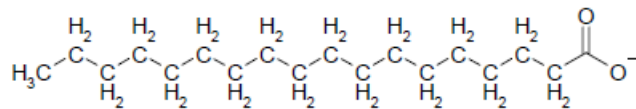


Figure 2-2: Molecular structure of soap (Turner, 2005)

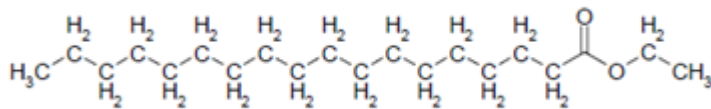


Figure 2-5 (b): Molecular structure of ethyl ester (Turner, 2005)

2.2 Feedstock for Biodiesel Production

Traditionally there are three main sources of feedstock for biodiesel production, which include vegetable oils (edible and non-edible), animal fats, and waste cooking oils. Examples of edible oils used as conventional biodiesel sources are rapeseed oil, sunflower oils, soybean oil, palm oil, coconut oil etc. However, taking into account the ever increasing human population and its proportional increase in edible oil consumption, the use of edible oils as a biofuel resource could result in starvation in developing countries (Janaun & Ellis, 2010). Henceforth, non-edible oils become a reasonable and promising alternative feedstock.

The major non-edible oil plants are soapnut, jatropha, karanja, tobacco, mahua, neem, rubber, sea mango, castor, cotton, etc. Of these feedstocks, jatropha, karanja, mahua, soapnut, and neem oils are the most often used in biodiesel production (Bankovic-Ilic *et al.*, 2012). The two types of non-edible oils used for this study are discussed in section 2.2.1.

2.2.1 Common non-edible Oils

➤ *Jatropha (Jatropha Curcas)*

By 2012 the annual production of the *Jatropha* plant in India was about 15kT. It is the most promising potential source for biodiesel synthesis in South-East Asia, Central and South America, India and Africa (Jain & Sharma, 2010). *Jatropha curcas* is a drought-resistant perennial that can grow almost anywhere on waste, sandy and saline soils, under different climates with minimal care (Karmakar *et al.*, 2010). It has a life cycle of 30-50 years thus eliminating the annual plantation.

Jatropha curcas species has oil content of about 37% that can be combusted as fuel without refining (Shika & Rita, 2012). It has properties comparable to those of mineral diesel such as calorific value and cetane number (Sirisomboon *et al.*, 2007). It has a great potential as an alternative fuel since it does not require any modification of the engine (Jain & Sharma, 2010). Depending on soil quality and rainfall, oil can be extracted from the *Jatropha* nuts

after two to five years. *Jatropha* is also suitable for preventing soil erosion and shifting of sand dunes (Kralova & Sjöblom, 2010).

➤ *Tobacco seed oil*

The mechanical properties (brake specific fuel consumption and brake thermal efficiency) of biodiesel manufactured from tobacco seed oil are similar to those of mineral diesel when tested in Single Cylinder Ci-Engine, with biodiesel having significantly lesser carbon monoxide and hydrocarbon emissions (Srinivas, *et al.*, 2013). The biodiesel synthesis from tobacco seed oil seems to be a feasible way for countries cultivating tobacco to break into a biofuels production market, thus contributing in combating greenhouse gas emissions caused by fossil fuels (Srinivas, *et al.*, 2013). Tobacco is mainly cultivated in Africa, Asia, southern and central Europe, Latin America, and Oceania (WHO, 2017). Tobacco seeds are produced in mass quantities during the cultivation of the plant therefore, there is sufficient feedstock for biodiesel production with tobacco plants being grown in over 4 million hectares of land in 125 countries worldwide (WHO, 2017) . Approximately 91% yield of biodiesel fatty acid methyl esters (FAME) having properties within diesel specifications is achieved in 30 minutes when pre-esterified tobacco seed oil (*Nicotiana tabacum* L.) is used. (Veljkovic', *et al.*, 2006)

South Africa has become a major producer of domestic tobacco, and although the majority of tobacco production is aimed at cigarette production, the opportunity of producing biodiesel using tobacco is now possible due to the Solaris project (Casey, 2015)

The South African biofuel market has particularly benefited from the cultivation of nicotine-free tobacco (Solaris seed tobacco) for the production of tobacco seed oil, that was blended with mineral jet fuel for a successful test flight with Boeing jets operated by South African Airways (SAA) in 2016 (ESI Africa, 2016).

2.3 Principles of Biodiesel Production

Non-edible oils can be used directly as fuel in diesel engine. However, direct use of non-edible oils poses significant engine operation issues in the long run. Problems such as injector chocking, ring sticking, wax formation, carbon deposits, misfire, ignition delay, and poor fuel atomization, are all attributed to high viscosity, low volatility, high flash point, and low cetane number of oil (Balat, 2011).

Properties of non-edible oils can be improved before injecting directly to the engine, thus preventing above mentioned problems. There are four ways to improve non-edible oil properties such as blending/ dilution, pyrolysis, micro-emulsion, and transesterification (Shika & Rita, 2012). These methods are described below;

i. Pyrolysis;

The chemical change resulting from application of thermal energy in the absence of air or nitrogen is called Pyrolysis. Vegetable oil is thermally decomposed to liquid oil fractions that are comparable to diesel fuels (Shika & Rita, 2012). The drawback, however, is that the product of oil from the pyrolysis reactor has lower viscosity, flash point, pour point, and cetane number than mineral diesel.

ii. Micro-emulsification;

Another way of solving the problem of highly viscous oils is through micro emulsions with a dispersant (co-solvency). Micro-emulsions are defined as transparent, thermodynamically stable colloidal dispersions ranging from 100 to 1000 Å (Shika & Rita, 2012). A micro-emulsion can be made of vegetable oils with an ester and dispersant (co-solvent), or of vegetable oils, an alcohol and a surfactant, and a cetane improver, with or without diesel fuels (Helwan *et al.*, 2009).

iii. Dilution/ Blending;

Dilution refers to the blending of vegetable oils with diesel fuel, solvent or ethanol to improve biodiesel properties and compatibility of biofuel with a diesel engine. Pre-combustion chamber engines with a mixture of 10% vegetable oil were used in Caterpillar, Brazil in 1980 in order to maintain the engine's total power without having to alter or adjust the engine (Shika & Rita, 2012). At that point it was not practical to substitute 100% vegetable oil for diesel fuel, but a blend of 20% vegetable oil and 80% diesel fuel was successful. Some short-term experiments used a blend of up to 50/50 ratio of vegetable oil and diesel fuel (Jaun *et al.*, 2011).

iv. Transesterification

Transesterification method has become the most accepted and widely used method for producing biodiesel. The transesterification works well when the starting oil is of high quality. However, quite often low quality oils are used as raw materials for bio-diesel

preparation. In cases where the FFA content of the oil is above 1%, difficulties arise due to the formation of soap which promotes emulsification during the water washing stage (using water); and at a FFA content above 3% the process becomes complex (Koh & Ghazi, 2011). A pretreatment step often termed pre-esterification is used for non-edible oils with high FFA content in order to reduce the FFA content. The next section discusses these reactions in detail.

2.4 Chemical Reactions involved

The reactions associated with biodiesel production include transesterification of triglycerides and esterification of free fatty acids (under acid catalysis), usually accompanied by potentially competing hydrolysis and saponification reactions.

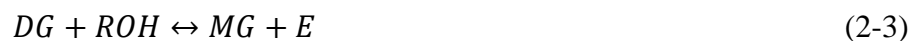
2.4.1 Transesterification Reaction

The common method to produce biodiesel from non-edible oils is transesterification of triglycerides with alcohol in the presence of either a base or strong acid catalyst. Chemical catalysts (base and acid) of alcoholysis can be homogeneous or heterogeneous. Non-catalytic alcoholysis reactions occur at high temperatures and pressures and still do not have any practical application (Bankovic-ilic *et al.*, 2012).

The transesterification reaction of triglycerides (TG) is as follows:



The transesterification reaction occurs in three steps as shown in equation (2-2) to (2-4). The triglyceride first reacts with alcohol to form a diglyceride and an alkyl ester. The diglyceride is then converted to monoglyceride thus releasing an additional alkyl ester, and lastly the monoglyceride is converted to glycerol, releasing a final alkyl ester.



Where, MG, DG, TG, and E stand for monoglyceride, diglyceride, triglyceride, and alkyl ester respectively

The alkyl esters produced depend on the type of alcohol used. Ethanol ($R=CH_2CH_3$) and methanol ($R=CH_3$) are common alcohols of choice. The choice of a catalyst is driven by factors such as the FFA content, fatty acid composition, economics and maximum product yield (Jaun *et al.*, 2011). There are three categories of catalysts that are often used in the transesterification of triglycerides, and these are homogeneous catalysts (acid or base), heterogeneous catalysts (acid or base), and enzymatic catalysts (Turner, 2005). The homogeneously and heterogeneously catalysed processes can either have one step or two steps (Bankovic-Ilic *et al.*, 2012). The latter process is recommended if a feedstock contains more than 1% of FFA (Ghadge & Raheman, 2005), although some authors have recently suggested the limit as 3% of FFA (Bankovic-Ilic *et al.*, 2012). Non-edible oils are usually high in FFA compared to edible oils, thus often limit the utilisation of highly effective base catalysts (Turner, 2005).

2.4.2 Homogeneously catalysed transesterification

Homogeneously catalysed transesterification is the most industrially applied method for biodiesel production from non-edible oil via one-step and two step processes (Bankovic-Ilic *et al.*, 2012). The choice of process (either one-step or two-step) is dependent mainly on the FFA content. For one-step process either an acid or base catalyst is used; with base catalysed transesterification reactions being economically feasible and having high catalytic activity and quality of the yield. However, the conversion of FFA to alkyl esters using a base catalyst becomes impossible due to the formation of soap. As a result, the soap formation decreases the yield of biodiesel and inhibits the separation of glycerol (Bankovic-Ilic *et al.*, 2012).

Several studies have conflicting results when it comes to the percentage yield of biodiesel, for example a study by da Silva *et al.* (2009) shows a 99% ester yield when castor oil and ethanol were used to produce biodiesel at 16:1 alcohol to oil molar ratio in the presence of sodium ethoxide catalyst. However, other studies report relatively lower yields, for instance studies by Chitra *et al.* (2005) and Deng *et al.* (2010) report low yields when jatropha oil was used. The difference in percentage yield of biodiesel is due to the difference in FFA content of different oils. The oil with low FFA content, alkyl ester yields of as high as 98% can be achieved in the presence of about 1% catalyst concentration under dry conditions to minimise soap formation (Bankovic-Ilic *et al.*, 2012). Sodium hydroxide (NaOH) and Potassium hydroxide (KOH) are commonly used base catalysts in base catalysed transesterification processes (Turner, 2005). The degree of conversion of triglycerides (TG) is highly influenced

by the initial catalyst concentration and the optimal catalyst concentration has been reported to be 1% based on oil weight (Bankovic-Ilic *et al.*, 2012).

Acid catalysed transesterification has many drawbacks, such as a slow reaction rate (by as much as 4000 times less than homogeneous base catalysed transesterification), minimal catalyst activity, high reaction temperature, and a high alcohol-oil molar ratio. Besides these disadvantages the use of acid catalyst in transesterification has some advantages; which include high tolerance towards high FFA content and the possibility of achieving both esterification and transesterification (Koh & Ghazi, 2011). Sulphuric acid (H_2SO_4), phosphoric acid (H_3PO_4), and hydrochloric acid (HCL), are among the most commonly used acid catalysts for transesterification.

Savaranan *et al.* (2010) conducted studies that gave biodiesel yield of approximately 90% using acid catalysed transesterification. However, both acid and base catalysed reactions had their limitations with base catalysed reactions having longer reaction times and acid catalysed reactions requiring higher temperatures (Saravanan *et al.*, 2010).

Due to the limitations of one-step process, the two-step process is normally preferred for non-edible oils with high FFA content. This process uses both acid and base catalysts with the first step being acid catalysed esterification of FFAs aimed at reducing the oil FFA content to less than 1% followed by a base catalysed alcoholysis in order to maximise the biodiesel production within a short period of time (Bankovic-Ilic *et al.*, 2012). Berchmans & Hirata (2008) found that 90% of fatty acid methyl esters were recovered whilst utilising the two-step process compared to the one step base catalysed process which gave 55% yield (Berchmans & Hirata, 2008). Table 2-1 shows results from several studies for a two-step homogeneously catalysed process using different non-edible oils.

Table 2-1: Two-step homogeneously catalysed process for different non-edible oils

(Bankovic-Ilic *et al.*, 2012)

A review of the two-step (acid/base) catalyzed homogeneously transesterification processes of different non-edible feedstocks (I – first step: acid pretreatment, II – second step: base-catalyzed).

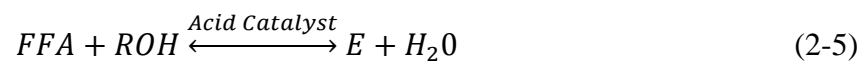
Feedstock (oil)	Type, volume of reactor, cm ³ /Type of agitator, agitation intensity, rpm	Step	Type of alcohol	Alcohol:oil molar ratio, mol/mol	Catalyst/loading, wt.% to the oil	Temperature, °C	Optimal reaction conditions	
							Reaction conditions	FFA conversion, %/Yield (conversion), %/Time, min
Jatropha	Glass tube, 15/Magnetic, 400	I	Methanol	0.2:1–0.4:1 ^a	H ₂ SO ₄ /1.3–1.6	60	1.43% H ₂ SO ₄ ^a	(92.8)/88
		II	Methanol	0.15:1–0.25:1 ^a	KOH/0.55 ^b	60	4:1 (0.16:1 ^a)	99/24
	Flask, –/Magnetic, 1000	I	Methanol	0.1:1–0.7:1 ^c	H ₂ SO ₄ /1	50	0.6:1 ^c	(93)/60
		II	Methanol	0.5:1–3.0:1	NaOH/1.4	65	ca. 6.7:1, 0.24:1 ^c	90/120
	Flask, –/Magnetic, 1000	I	Methanol	3:1–12:1	H ₂ SO ₄ /0.3–2	40–100	45 °C, 6:1, 0.5% H ₂ SO ₄ ,	(93)/120
		II	Methanol	3:1–12:1	KOH/0.5–2.0	60	60 °C, 9:1, 2% KOH	95/120
	Batch reactor, 1500/–, 400	I	Methanol	3:1–9:1	H ₂ SO ₄ /0.25–1.5	40–100	45 °C, 6:1, 0.5% H ₂ SO ₄	(93)/120
		II	Methanol	3:1–9:1	KOH/0.5–2.0	40–100	60 °C, 9:1, 2% KOH	95/120
	Flask, 500/Mechanical, 600	I	Methanol	2.8–2:3 ^a	H ₂ SO ₄ /0.5–3	20–80	65 °C, 3.7 ^a , 1% NaOH ₄ ,	(95)/180
		II	Methanol	3:7 ^a	NaOH/0.5–3	20–80	50 °C, 3.7 ^a , 1% NaOH	90.1/180
	Flask, 1000/Mechanical, 600	I	Methanol	0.16:1–0.48–1 ^a	H ₂ SO ₄ /1–6 ^a	60	0.4:1 ^a , 4% H ₂ SO ₄ ^a	(88.5)/60
		II	Methanol	0.16:1–0.48–1 ^a	NaOH/0.8–1.6	60	0.24–1 ^a , 1.4% NaOH	96.4 ^a /30
	Stock tank, 50	I	Methanol	8:1–10:1	H ₂ SO ₄ /0.2–1.0	60	8:1, 0.4% H ₂ SO ₄	(92)/30
		II	Methanol	6:1	KOH/0.6–1.2	60	6:1, 1% KOH	86.2/30
Jatropha ^f	Batch reactor, –/Mechanical, –	I	Methanol	0.16:1–0.4:1 ^a	H ₂ SO ₄ /1–4 ^a	–	0.32:1, 3% H ₂ SO ₄ ^a	(91.4)–
		II	Methanol	8:1	NaOH/1.2	–	–	(99.38) ^f /10
Karanja	Flask, –/Magnetic, 1000	I	Methanol	3:1–9:1	H ₂ SO ₄ /0.25–2	40–80	50 °C, 6:1, 1% H ₂ SO ₄	(94)/45
		II	Methanol	3:1–9:1	KOH/0.3–1.0	40–80	50 °C, 9:1, 0.5% KOH	80/30
	Flask, –/Teflon stirrer, 300	I	Methanol	6:1	H ₂ SO ₄ /0.5	65	–	(91)–
		II	Methanol	6:1	KOH/1	65	–	97–
	Jacketed reactor, 1000/Digital stirrer, 600–650	I	Methanol	0.1:1–0.5:1 ^c	H ₂ SO ₄ /0.5–5	–	33.83:1 ^c , 3.73% H ₂ SO ₄	(81.8)/3.17
		II	Methanol	0.1:1–0.5:1 ^c	KOH/0.5–1.5	–	9.3:1 (33.4:1 ^c), 1.33% KOH	89.9 ^c /2.5
Mixture of mahua and simarouba	Cimbal flask, 250/–, 230	I	Methanol	Mahua oil: 0.34–0.36 ^a	H ₂ SO ₄ /1.4–1.49 ^a	–	19.37:1, 14.38%	–/59–90
				Simarouba oil: 0.27–0.40 ^a	H ₂ SO ₄ /1.4–1.54 ^a	–	–	–/40–90
Kusum	Flask, 1000/Mechanical, 1200	I	Methanol	5:1	KOH	60	–	98/30
		II	Methanol	6:1–12:1	H ₂ SO ₄ /0.5–1.25 ^a	40–64	50 °C, 10:1, 1% H ₂ SO ₄ ^a	(96)/60
Tobacco	Flask, –/Magnetic, 400	I	Methanol	6:1–12:1	KOH/0.5–1.1	40–65	50 °C, 8:1, 0.7% KOH	95/60
		II	Methanol	4.5:1–18:1	H ₂ SO ₄ /1–2	60	13:1, 2% H ₂ SO ₄	(94)/50
Castor	Flask, 100/Magnetic, 300	I	Ethanol	6:1	KOH/1	60	–	91/30
		II	Ethanol	40:1	H ₂ SO ₄ /1	60	–	–/60
	Flask, 100/Magnetic, 300	I	Ethanol	20:1	KOH/1	60	–	(95.3)/60
		II	Ethanol	40:1	H ₂ SO ₄ /1	60	–	–/60
Palm/rubber blend (1:1)	Flask, –/–, 360	I	Ethanol	20:1	KOH/1	60	–	(95.6) ^b /60
		II	Methanol	6:1–10:1	KOH/0.5–2	45–65	55 °C, 8:1, 2% KOH	(96)/3
Datura stramonium		I	Methanol	6:1–10:1	H ₂ SO ₄ /0.4–1	60	8:1, 0.6% H ₂ SO ₄	(89)/30

2.4.3 Heterogeneously catalysed transesterification

Using a solid base catalyst has proven to be environmentally friendly as it provides a simpler means of recovery and purification (Bournay, 2005). This in turn results in the reduction of the amount of waste water. Furthermore these catalysts can be regenerated for reuse in the process thus reducing operational costs. However, catalyst preparation is complex and diffusion inhibitions associated with the three phase mixture result in slow reaction rates (Meher *et al.*, 2006). Like homogeneously catalysed transesterification, the type of catalyst used is dependent on the FFA content of the non-edible oil (Bankovic-Ilic *et al.*, 2012). Solid acid catalyst is commonly used for the synthesis of fatty acid methyl esters from non-edible oils due to their ability to simultaneously perform esterification and alcoholysis (Lopez *et al.*, 2007). There have been challenges in developing these with a completely heterogeneously catalysed two-step process (Bankovic-Ilic *et al.*, 2012).

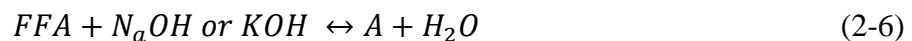
2.4.4 Esterification Reaction

An esterification reaction is an acid catalysed conversion of FFAs into alkyl esters. Esterification reaction is sometimes performed as a pre-treatment step for non-edible oils with high FFA content before base catalysed transesterification and it is also a resultant reaction for acid catalysed transesterification (Wang, 2007). Equation (2-5) shows the esterification of FFA to produce an alkyl ester and water. When used as a pre-treatment step in the presence of 2% ferric sulphate catalyst, 97% conversion of waste cooking oil with high FFA content was achieved in the study conducted by Wang *et al.* (2007)



➤ Side Reactions: Saponification and Hydrolysis

Depending on the quality of the non-edible oil, undesired side reactions may occur. Non-edible oil with excessive FFA content will be neutralised with excess base (NaOH or KOH) resulting in side reactions such as saponification and hydrolysis (Yazdani & Gonzalez, 2007). A saponification reaction produces soap and water as shown in equation (2-6). During the saponification reaction water reacts with an alkyl ester under base catalysis to form FFA and alcohol as shown in equation (2-7).



Where: E stands for alkyl ester, and A stands for Soap

2.5 Transesterification thermodynamics and reaction kinetics

Determining the reaction rate and phase separation kinetics requires the knowledge of thermodynamic properties of biodiesel and reactants. Generally the thermodynamic properties of biodiesel differ from those of petroleum diesel or gasoline, for example boiling point, pour point, flash point, and cloud point of biodiesel is relatively higher than petroleum diesel, gasoline, and that of alcohols (Lotero, 2005). High flash point is required for safe handling of the fuel (ASTM, 2005). Table 2-2 shows the thermodynamic properties of biodiesel compared to petroleum diesel, gasoline and alcohols. As can be seen from the table, density and viscosity of biodiesel is higher.

Table 2-2: Physical Properties of Diesel and Biodiesel Fuels

(Source: Adapted from (Lotero, 2005); (Brown, 2003); (ASTM, 2005); (Encinar *et al.*, 2005); and (Barnwal & Sharma, 2005))

Propert (ASTM)	Units	Diesel (no.2)	Biodiesel (general)	Sunflower ME	Rapeseed ME	Soy ME	Sunflower EE	Rapeseed EE	Soy EE	Gasoline	Ethanol	Methanol
Viscosity (D445)	$\nu(40^{\circ}\text{C})$ (cSt)	1.9-4.1	1.9 - 6	4.2 - 4.6	4.8	4.1-4.5	4.5	-	4.4	0.8	1.5	0.75
Density (D4052)	R(25°C) (g/ml)	0.85	0.88	0.86	0.89	0.89	0.87	0.87	0.88	0.72-0.78	0.794	0.796
Boiling Point	BP (°C)	210-235	-	-	-	339	-	-	-	30-255	78	65
Flash Point (D93A)	FP (°C)	60-80 (52)	100- 70	164-183	153	141-188	187	191	195	-43	13	11
Cloud Point (D2500)	CP (°C)	-19 to 5	-3 to 12	-3	-3	2	-1	8	1	-	-	-
Pour Point	PP (°C)	-35 to -15	-15 to 16	-6	-	-2	-8	-	-4	-	-	-
Combustion Point	CBP (°C)	95^2	-	183	-	171	192	-	-	-	-	-
Autoignition temperature	AIT (°C)	254	-	-	-	-	-	-	-	370	370	464
Distillation (D86)	50% (°C)	-	-	-	-	-	353	-	344	-	-	-
Cetane Index (D4737)	CI	40 - 55	48 -60	49	52	45-47	49.4	-	48.2	<15	<15	<15
Octane Number	-	-	-	-	-	-	-	-	-	82-92	90-102	89-102
Lubricity (D6079)	HFRR (μm)	685	314	-	-	-	-	-	-	-	-	-
Lubricity	BOCLE (g)	3600	>7000	-	-	-	-	-	-	-	-	-
Higher heating value	HHV (MJ/kg)	45.2	-	40.1	40	40	38.9	38.7	40	43.5	27	20.1
Heat of vaporisation	HV (kJ/kg)	375	-	-	-	-	-	-	-	380	920	1185
Water	%vol	0.05	0.05	-	-	-	-	-	-	-	-	-
Carbon (D189)	wt%	87	77	-	-	-	-	-	-	-	-	-
Hydrogen	wt%	13	12	-	-	-	-	-	-	-	-	-
Oxygen	wt%	0	11	-	-	-	-	-	-	-	-	-
Sulphur (D4294)	wt%	0.05	0.05	0.01	<0.01	0.01	<0.01	-	0.1	-	-	-
Ramsbottom residue	%	0.14	-	-	-	-	0.3	-	0.69	-	-	-

2.5.1 Reaction kinetics

Reaction kinetics pertains to the rate of chemical reactions (reversible or irreversible). The kinetics for biodiesel production is largely dependent on the phase, reaction temperature, reactant concentration, and the type of catalyst used to lower the activation energy needed to start a reaction (He *et al.*, 2007).

Rate equations are expressed in terms of reactant concentrations and are typically obtained by use of the law of mass action (LMA). LMA states that the rate of reaction is directly proportional to the products of reactant concentrations, each raised to the power of its

coefficient in the reaction. The law only applies to elementary reactions; those depicting the mechanism at the molecular level, and occurring as a single event (Turner, 2005). Simplicity tests are used to predict the order of the reaction, however these tests still need to be verified by experiment (Turner, 2005). Below are reactions of saponification, hydrolysis and transesterification and their rate equations under LMA.

Saponification reaction



Where k_{12} is the reaction rate constant

Saponification rate equation

$$\frac{dW}{dt} = k_{12}[FFA]^1[OH^-]^1 \quad (2-9)$$

Hydrolysis reaction



The hydrolysis reaction is a reversible reaction, meaning it can proceed in either forward or backward direction depending on reaction conditions. The forward reaction rate is controlled by the reaction rate constant k_1 , and the reverse reaction is governed by k_{1r} . When the rate of the forward reaction is the same as that of the reverse reaction, the reversible reaction is said to be in equilibrium. The equilibrium constant is given by equation (2-11) below

$$K_1 = \frac{k_1}{k_{1r}} = \frac{[RO^-][H_2O]}{[ROH][OH^-]} \quad (2-11)$$

Transesterification

Taking the first forward reaction of transesterification, as given by equation (2-2) and applying LMA, the rate equation for transesterification of TG is found to be;

$$-\frac{d[TG]}{dt} = k_1[TG][ROH] \quad (2-12)$$

The reaction kinetics of biodiesel production changes with system temperature and pressure. According to Freedman *et al.* (1986), transesterification follows pseudo first-order kinetics and the reverse reaction occurs as described by second-order kinetics. For methanol

approximating at its critical point, Warabi *et al.* (2004) considered kinetics to be first-order as described by equation (2-13).

$$-\ln \frac{x_t}{x_0} = kt \quad (2-13)$$

Where x_t is the concentration of unreacted methyl esters at time t ; x_0 is the initial methyl ester concentration; k is the first-order reaction rate constant.

The determination of reaction constant is necessary for the determination of activation energy required for the reaction to occur. Reaction constants are a function of temperature and are obtained by taking the slope of the plot $\ln(k)$ vs $1/T$. The activation energy is then determined from the Arrhenius equation given in equation (2.14).

$$\ln k = \ln A - \frac{E_a}{RT} \quad (2-14)$$

Where E_a is the activation energy; R is the universal gas constant; T is temperature.

2.6 Kinetic Models

Kinetic models are necessary in predicting the extent of reactions that occur during the production of biodiesel and they also allow for optimization of process variables for better efficiency. Although the production of biofuels has become rather crucial in the current trying times of the depletion of fossil fuel reserves and many other related challenges such as stricter air emissions standards, the kinetics of transesterification remain controversial. Two widely accepted kinetic models have been developed and will be discussed in the following sections.

2.6.1 Freedman's Kinetic Model

Freedman and his colleagues devised a chemical kinetic model for the alcoholysis of soy bean oil in the early 1980's at USDA and they used the overall reaction of TG to alkyl esters (equation 2-1) which occurs as a sequence of three steps as shown by equations (2-2) to (2-4) in section 2.4.1.

Freedman's model seems to be devised from the LMA, because the first forward reaction proceeds according to equation (2-12). The overall order of the proposed forward reaction step is second-order and a condition called pseudo-first order occurs when the concentration of alcohol is assumed constant due to the very high molar ratio of alcohol to the TG (Freedman *et al.*, 1986).

The aim of most kinetic models is to find the best fit of empirical data to models of simple reaction order; when the data doesn't fit Freedman suggests what is called a shunt reaction, which is a fourth-order reaction in which three alcohol molecules concurrently react with a TG (Freedman *et al.*, 1986). The shunt reaction correlates to;

$$[TG][ROH]^3 \quad (2-15)$$

Freedman studied the transesterification of soy bean oil using methanol and butanol with alcohol to oil ratios of 30:1 and 6:1 at temperatures varying from 20 degrees Celsius to 60 degrees Celsius (Freedman *et al.*, 1986). Reverse reactions for the transesterification of soy bean oil were found to be second order for both methanol and butanol. When using butanol, the forward reactions were found to be second order at 6:1 alcohol to oil molar ratio, and pseudo-first-order at 30:1 alcohol to oil molar ratio. With methanol, the forward reactions were fourth order (shunt reaction) at 6:1 alcohol to oil molar ratio, and pseudo-first-order at 30:1 alcohol to oil molar ratio (Freedman *et al.*, 1986).

The Arrhenius equation (equation 2-14) was used to find the rate constants and ultimately the activation energies by taking the slope of $\ln(k)$ vs. $1/T$. There have been several investigations that used the application of the Freedman kinetic model. One study was conducted by Mittelbach, (1990) at the University of Karl Franzen University, Austria and it was found that the reaction was not a single phase as previously suggested by Freedman, but that for the first two minutes a two phase system was observed. Another discrepancy found by Mittelbach, (1990) is that the reaction order of the forward reactions is not governed by second-order kinetics.

Another application of Freedman's kinetic model was by Nouredini *et al.*, (1997) when they studied the kinetics of the transesterification of soybean oil with methanol. These researchers particularly focused on studying the effect of mixing and agitation by measuring the Reynolds number of the stirrer and they found that the reaction constants for the shunt reaction were negligibly small for there to be a correlation of the data to the shunt reaction.

An investigation by Bikou *et al.*, (1999) focused on the study of the effect of water on the kinetics of the transesterification of cotton oil with ethanol under the catalysis of potassium hydroxide. Contrast to Freedman's kinetic model, Bikou *et al.*, (1999) found that each of the three transesterification reaction steps were third order with respect to methanol.

It is evident that Freedman's kinetic model doesn't always correlate with the other studies that have been done since its inception, and additionally it doesn't take into account the effect of water on transesterification -which has a huge impact as discussed by Bikou *et al.*, (1999). There is also concern with the formation of saponification when performing transesterification under base catalysis and a superior predictive model should take that into account; this then consequently leads to the discussion of Komers' kinetic model.

2.6.2 Komers' Kinetic Model

Komers' model is based on the transesterification of vegetable oil using methanol as a solvent and potassium hydroxide (KOH) as catalyst. Komers and his colleagues built a model from suggested mechanisms for all the competing reactions (saponification, methanolysis, and methoxide formation) that occur during transesterification and is the only model that explicitly treats the amount of water and catalyst present (Komers, 2002). The research on the negative effect of water on the equilibrium reactions by Bikou *et al.*, (1999) is supported by this model.

Komers proposed simplifying assumptions that resulted in a system of six rate equations including eight reaction species and ten rate constants (Komers, 2002). The simplifying assumptions are listed below;

- a) The concentration of FFAs is negligible
- b) Of all the theoretically possible reactions only two progress to form products: the alcoholysis of acylglycerols (TAG, DAG, MAG) and the saponification of TAG, DAG, MAG, or alkyl esters (E).
- c) All the isomers of TAG, DAG, MAG, and E proceed at the same rate, with the same mechanism.
- d) Alcoholysis is catalysed by OH^- or RO^- (alkoxide) ions. Concentrations of OH^- and RO^- ions are much smaller than those of TAG and ROH.

The abovementioned assumptions give rise to the differential equations below (The derivation for Komers model is found in appendix A).

$$-\frac{dTAG}{dt} = b \cdot OH \cdot (k'_2 \cdot TAG \cdot ROH - k'_{2r} \cdot DAG \cdot E) + a \cdot OH \cdot k_9 \cdot TAG \quad (2-16)$$

$$-\frac{dDAG}{dt} = b \cdot OH \cdot (-k'_2 \cdot TAG \cdot ROH + k'_{2r} \cdot DAG \cdot E + k'_4 \cdot DAG \cdot ROH - k'_{4r} \cdot MAG \cdot E) + a \cdot OH \cdot (-k_9 \cdot TAG + k_{10} \cdot DAG) \quad (2-17)$$

$$-\frac{dMAG}{dt} = b \cdot OH \cdot (-k'_4 \cdot DAG \cdot ROH + k'_{4r} \cdot MAG \cdot E + k'_6 \cdot MAG \cdot ROH - k'_{6r} \cdot G \cdot E) + a \cdot OH \cdot (-k_{10} \cdot DAG + k_{11} \cdot MAG) \quad (2-18)$$

$$\frac{dG}{dt} = b \cdot OH \cdot (k'_6 \cdot MAG \cdot ROH - k'_{6r} \cdot G \cdot E) + a \cdot OH \cdot k_{11} \cdot MAG \quad (2-19)$$

$$-\frac{dROH}{dt} = \frac{dE}{dt} = b \cdot OH \cdot (k'_2 \cdot TAG \cdot ROH - k'_{2r} \cdot DAG \cdot E + k'_4 \cdot DAG \cdot ROH - k'_{4r} \cdot MAG \cdot E + k'_6 \cdot MAG \cdot ROH - k'_{6r} \cdot G \cdot E - k_8 \cdot E) \quad (2-20)$$

$$-\frac{dOH}{dt} = \frac{dA}{dt} = b \cdot OH \cdot k_8 \cdot E + a \cdot OH \cdot (k_9 \cdot TAG + k_{10} \cdot DAG + k_{11} \cdot MAG) \quad (2-21)$$

$$-\frac{dH_2O}{dt} = \frac{dFFA}{dt} = a \cdot k_{12} \cdot FFA \cdot OH \quad (2-22)$$

Where $a = [TAG]_0$ and $b = [ROH]_0$

2.6.3 Other Models

There are various other studies that investigated the transesterification of oil for biodiesel synthesis, under catalytic and non-catalytic conditions. Below is a summary of different kinetic models, some of which are not discussed into detail in this paper (Liu, 2013).

Table 2-3: Summary of different kinetic models (Liu, 2013)

Model	Reactions	Order	Ref.
Three steps, reversible, alkaline as catalyst	$TG + MeOH \xrightleftharpoons[k_{-1}]{k_1} DG + ME$ $DG + MeOH \xrightleftharpoons[k_{-2}]{k_2} MG + ME$ $MG + MeOH \xrightleftharpoons[k_{-3}]{k_3} GL + ME$	Second order	(Darnoko & Cheryan, 2000, Noureddini & Zhu, 1997, Wenzel et al., 2006, Shahbazi, M.R., et al., 2012)
Three steps, irreversible, no catalyst	$TG + MeOH \xrightarrow{k_1} DG + ME$ $DG + MeOH \xrightarrow{k_2} MG + ME$ $MG + MeOH \xrightarrow{k_3} GL + ME$	First order	(Diasakou et al., 1998)
One step, reversible, non catalyst	$TG + 3MeOH \xrightleftharpoons[k_{-1}]{k_1} GL + 3ME$	First order	(Kusdiana & Saka, 2001, He et al., 2007)
One step reversible, different base catalysts	$TG + 3MeOH \xrightleftharpoons[k_{-1}]{k_1} GL + 3ME$	First order, or third order, depends on catalyst type	(Singh & Fernando, 2007)

TG: triglyceride. MeOH: methanol. DG: diglyceride. MG: monoglyceride. GL: glycerol. ME: methyl esters.

2.7 Parameters that influence the transesterification reaction

Transesterification is influenced by various parameters such as fatty acid concentration, FFA content of the oil, reaction temperature, ratio of alcohol to vegetable oil, catalyst, mixing intensity, purity of reactants, and water content amongst others (Wang *et al.*, 2011). Some of the influencing parameters are discussed in detail in the following sections;

2.7.1 Reaction Temperature

Reaction temperature significantly influences the rate of reaction. However literature suggests that if given enough time, the reaction can still proceed to a near completion at room temperature (Karmakar *et al.*, 2010). Commonly the reaction starts near boiling point of the

alcohol under atmospheric conditions. To proceed successfully, the removal of FFA from the oil by refining or pre-esterification is imperative (Bankovic-Ilic *et al.*, 2012).

Further increase in temperature is reported to have a negative effect on the conversion. Literature has indicated that if given enough time, transesterification can proceed satisfactorily at ambient temperatures in the presence of the alkaline catalyst. It was observed that bio-diesel recovery was affected at very low temperatures but conversion was almost unaffected (Shahid & Jamal, 2010).

2.7.2 Alcohol to Oil Molar Ratio

The stoichiometry of the transesterification reaction requires 3 moles of alcohol per mole of triglyceride to give 3 moles of fatty esters and 1 mole of glycerol. To shift the transesterification reaction to the right, it is necessary to use either a large excess of alcohol or to remove one of the products from the reaction mixture (Shika & Rita, 2012). When 100% excess alcohol is used, the reaction rate is at its highest. Higher molar ratio of alcohol to oil interferes in the separation of glycerol. It was observed that lower molar ratios required more reaction time. With higher molar ratios, conversion increased but recovery decreased due to poor separation of glycerol. It was found that optimum molar ratios depend upon type and quality of oil (Vyas *et al.*, 2010).

2.7.3 Catalyst Type and Concentration

Alkali metal alkoxides are the most effective transesterification catalyst compared to the acidic catalysts. Sodium alkoxides are among the most efficient catalysts used for this purpose. Transmethylation occurs approximately 4000 times faster in the presence of an alkaline catalyst than those catalyzed by the same amount of acidic catalyst (Bankovic-Ilic *et al.*, 2012). Partly for this reason and because alkaline catalysts are less corrosive to industrial equipment than acidic catalysts, most commercial transesterification are conducted with alkaline catalysts. Further, increase in catalyst concentration does not increase the conversion and it adds to extra costs because it is necessary to remove it from the reaction medium at the end (Shika & Rita, 2012). It was observed in literature that higher amounts of sodium hydroxide (NaOH) catalyst were required for higher free fatty acid oil (Janaun & Ellis, 2010).

2.7.4 Purity of Reactants

Impurities present in the oil also affect conversion levels. Under the same conditions, 67 to 84% conversion of oil into esters using crude oils can be obtained, when compared with 94 to 97% conversion using refined oils (Shika & Rita, 2012). The free fatty acids in the original oils interfere with the catalyst and under conditions of high temperature and pressures this problem can be overcome (Janaun & Ellis, 2010). It was observed that crude oils were equally good compared to refined oils for production of bio-diesel. However, the oils should be properly filtered (Kumar & Sharma, 2011).

2.7.5 Mixing Intensity

The mixing is most significant during the slow rate region of the transesterification reaction. As the single phase is established, mixing becomes insignificant. The understanding of the mixing effects on the kinetics of the transesterification process is a valuable tool in the process scale-up and design. It was observed in literature that after adding alcohol and catalyst to the oil, 5-10 minutes stirring helps in higher rate of conversion and recovery (Kumar & Sharma, 2011).

2.7.6 Effect of Alcohol Type

Methanol gave the best biodiesel yield, followed by butanol and least was with ethanol. There are many reasons behind it. Firstly, Methanol has a simple chemical structure, thus the transesterification reaction is more likely to occur (Shika & Rita, 2012). Butanol and ethanol are more complex; therefore it is more difficult for transesterification to occur (Shika & Rita, 2012). Secondly, with methanol, the emulsions form quickly and easily breaks down to form a lower glycerol rich layer and upper methyl ester rich layer. When using ethanol, the emulsions are more stable and severely complicate the separation and purification of esters (Jain & Sharma, 2010).

2.7.7 Effect of Reaction Time

The conversion of oil to biodiesel reaches equilibrium conversions with increased reaction times. The maximum ester conversion is obtained at 2 hour reaction time. Similar reaction time has been reported in Mahua (*Madhuca Indica*) and Karanja oil. The reaction is very slow during the first minute due to mixing and dispersion of methanol into catalyst. From 1 to 5

minute(s), the reaction proceeds very fast. The production of beef tallow methyl esters reaches the maximum value at about 15 minutes (Kumar *et al.*, 2012).

2.7.8 Effect of Moisture and Water Content on the Yield of Biodiesel

Water could pose a greater negative effect than presence of FFA and hence the feedstock should be free from water. Even a small amount of water (0.1%) in the transesterification reaction would decrease the ester conversion from vegetable oil. The yield of the alkyl ester decreases due to presence of water and FFA as they cause soap formation, consume catalyst and reduce the effectiveness of catalyst (Shika & Rita, 2012).

2.7.9 Effect of Free Fatty Acids

FFAs content after acid esterification should be minimal or otherwise less than 2% FFAs. These FFAs react with the alkaline catalyst to produce soaps instead of esters. There is a significant drop in the ester conversion when the free fatty acids are beyond 2% (Silitonga *et al.*, 2011).

2.8 Optimization of non-edible oil transesterification

Biodiesel yield depends on the reaction conditions, including the ones detailed in section 2.3.4; therefore optimization of these conditions is crucial in order to determine the optimal conditions for maximum biodiesel yield of the highest purity. Catalyst loading, alcohol to oil molar ratio, and their interactions have a significant impact on the yield of alkyl esters (da Silva *et al.*, 2009). Supporting the previous statement is a study conducted by Cavalcante *et al.*, (2010) stating that the ethanol to castor oil molar ratio, reaction time, and potassium hydroxide catalyst loading are effective on the alkyl ester yield in both the linear and quadratic model at 95% confidence level.

Design of experiments is a statistical technique that offers an efficient and accurate way of optimizing processes. Examples of this technique are, the response surface methodology (RSM) combined with the central composite rotatable design, factorial design, Box-Behnken factorial design or the combination of fractional factorial and Doerhlert experimental design, as well as Taguchi technique and generic algorithm coupled with artificial neural network (Bankovic-Ilic *et al.*, 2012). These techniques not only assess the influence of individual process parameters but also the interactions between them.

CHAPTER 3

3. Methodology

This research project comprised of five stages:

a) Stage 1: Response surface methodology (RSM) was performed to assess the influence of operating parameters at different conditions.

b) Stage 2: Optimisation of the model obtained from RSM was done to obtain the optimum operating conditions.

c) Stage 3: Concentration-time data for catalysed transesterification of biodiesel was collected from literature in order to fit into a kinetic model found in literature.

d) Stage 4: To find the true order of reactions, the concentration-time data was fitted into the rate equation and rate constants were estimated. A robust optimisation solver which minimized the objective function was applied to obtain optimised values of the rate constants. Such an objective function is given by Equation (3-1)

$$E^2 = \sum_{i=1}^n [b_i - (a_{i1}k_1 + a_{i2}k_2 + a_{i3}k_3 + \dots + a_{in}k_n)]^2 \quad (3-1)$$

Statistical regression techniques were employed for fitting the model, and the developed model went through the steps as depicted by figure 3.1.

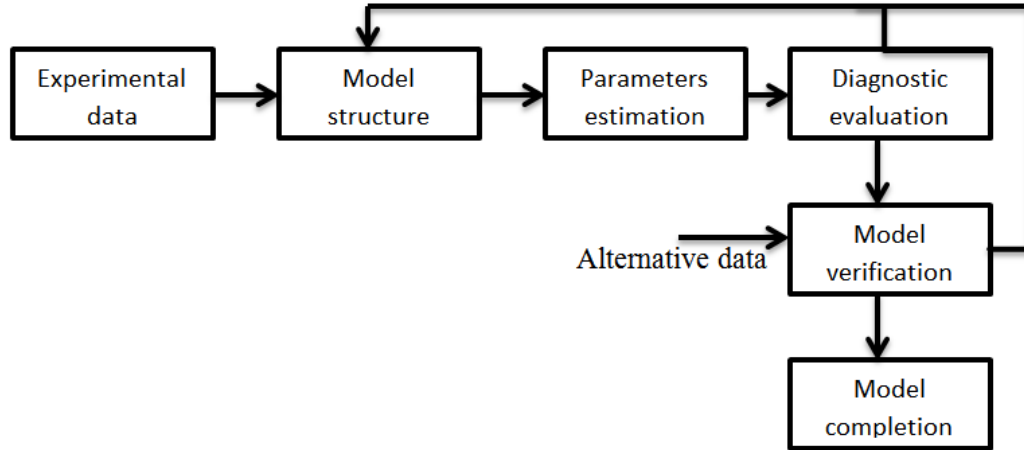


Figure 3-1: Model validation structure

3.1. Derivation of theoretical kinetic model

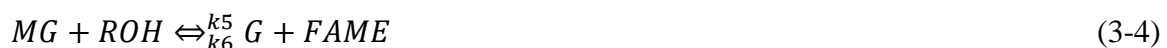
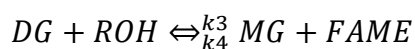
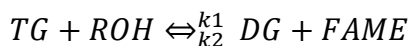
For the purpose of this study, a theoretical kinetic model from literature (Noureddini & Zhu, 1997) that represents the production of biodiesel from non-edible oils is proposed. Theoretically biodiesel fatty methyl esters are produced as a result of transesterification reaction involving a 3:1 alcohol to oil molar ratio. The overall reaction for biodiesel reaction is given by equation (3-2) below.



There are instances where alcohol is fed in excess in order to achieve higher reagent conversions. In such instances equation (3-2) behaves as an irreversible reaction (equation 3-3).



The overall reaction occurs in three consecutive steps (equation 3-4), a 3-step reversible reaction with alkaline as a catalyst. The reaction is assumed to be first order with respect to reacting species and second order overall.



Where k_1 , k_3 , and k_5 are forward rate constants, and k_2 , k_4 , and k_6 are reverse rate constants.

The model above is governed by the following assumptions:

- The concentration of FFAs is negligible
- Of all the theoretically possible reactions only one reaction progresses to form products: the alcoholysis of triglycerides (TG, DG, and MG).
- The alcoholysis of triglycerides assumes that elementary rate law applies.
- Alcoholysis is catalysed by RO^-/OH^- ions.
- Reaction rate is dependent only on temperature, and the reaction rate constant is correlated by the Arrhenius equation.
- The volume of the batch reactor does not change appreciably during the course of the chemical reaction ($V_0 = V$).

Performing component mass balance, results in the following ordinary differential equations:

$$\frac{dC_{TG}}{dt} = -k_1 \cdot [C_{TG}]_t \cdot [C_{ROH}]_t + k_{1r} \cdot [C_{DG}]_t \cdot [C_E]_t$$

$$\frac{dC_{DG}}{dt} = k_1 \cdot [C_{TG}]_t \cdot [C_{ROH}]_t - k_{1r} \cdot [C_{DG}]_t \cdot [C_E]_t - k_2 \cdot [C_{DG}]_t \cdot [C_{ROH}]_t + k_{2r} \cdot [C_{MG}]_t \cdot [C_E]_t$$

$$\frac{dC_{MG}}{dt} = k_2 \cdot [C_{DG}]_t \cdot [C_{ROH}]_t - k_{2r} \cdot [C_{MG}]_t \cdot [C_E]_t - k_3 \cdot [C_{MG}]_t \cdot [C_{ROH}]_t + k_{3r} \cdot [C_G]_t \cdot [C_E]_t$$

$$\frac{dG}{dt} = k_3 \cdot [C_{MG}]_t \cdot [C_{ROH}]_t - k_{3r} \cdot [C_G]_t \cdot [C_E]_t$$

$$\frac{dC_E}{dt} = -k_{1r} \cdot [C_{DG}]_t \cdot [C_E]_t + k_1 \cdot [C_{TG}]_t \cdot [C_{ROH}]_t - k_{2r} \cdot [C_{MG}]_t \cdot [C_E]_t + k_2 \cdot [C_{DG}]_t \cdot [C_{ROH}]_t - k_{3r} \cdot [C_G]_t \cdot [C_E]_t + k_3 \cdot [C_{MG}]_t \cdot [C_{ROH}]_t$$

$$\frac{dC_{ROH}}{dt} = -\frac{dC_E}{dt} \tag{3-5}$$

3.2. Kinetic Parameters

The estimation of activation energy is obtained from the Arrhenius correlation (equation 3-6) by plotting $\ln(k)$ vs $1/T$, where E_a/R is the slope.

$$\ln k = \left(\frac{E_a}{RT} \right) + \ln k_0 \quad (3-6)$$

Where E_a =activation energy (J/mol), R = universal gas constant (8.314J/mol/K), k_0 = pre-exponential factor (1/time unit).

CHAPTER 4

4. Results and Discussion

4.1 Kinetic models and Response surface methodology

4.1.1 Response Surface Methodology

To understand the influence of operating parameters on biodiesel yield from *Jatropha curcas* oil, experimental data was obtained from Pedavoah, (2010). Experiments were conducted at various conditions, varying temperature, molar ratio, reaction time, catalyst amount, and stirring rate. Surface response plots were generated for variations in reaction time, stirring rate, and temperature whilst keeping molar ratio and catalyst amount constant. Alcohol to oil molar ratio was kept at 6:1 and catalyst amount to 0.6g (1%/w oil). Experimental data is found in Appendix B. Table 4.1 and 4.2 below show the parameters for the 2^3 full factorial design.

Table 4-1: 2^3 Design summaries

Factor	Name	Units	Actual low	Actual high	Coded low	Coded high
X1	Temperature	[$^{\circ}$ C]	45	85	-1	+1
X2	Time	[min]	15	60	-1	+1
X3	Stirring rate	[rpm]	0	500	-1	+1

Table 4-2: Design matrix

X1:Temperature	X2:Time	X3:Stirring rate	Yield (vol %)
1	1	1	74.1
1	1	-1	86.11
-1	1	-1	87.04
-1	-1	-1	87.04
1	-1	1	81.79
-1	-1	1	79.23
1	-1	-1	83.02
-1	1	1	76

Several linear and quadratic polynomial models were generated using MATLAB® Ver. R2012b and were fitted with experimental data in order to obtain the equation of best fit. The 1st order polynomial model that best fit the data with minimal deviation to experimental data and correlation factor of 0.89 was found to be:

$$Y = 99.0887 - 0.1072 * X1 - 0.1305 * X2 - 0.016 * X3 + e \quad (4-1)$$

Where e= mean error

Table 4-3: Variance analysis

Mean error	Variance residual	R ²
-.27711e-13	5.1184	0.89

Figure 4.1 shows the comparison between actual and predicted yield. As can be seen from the figure, the model closely predicts the actual biodiesel yield.

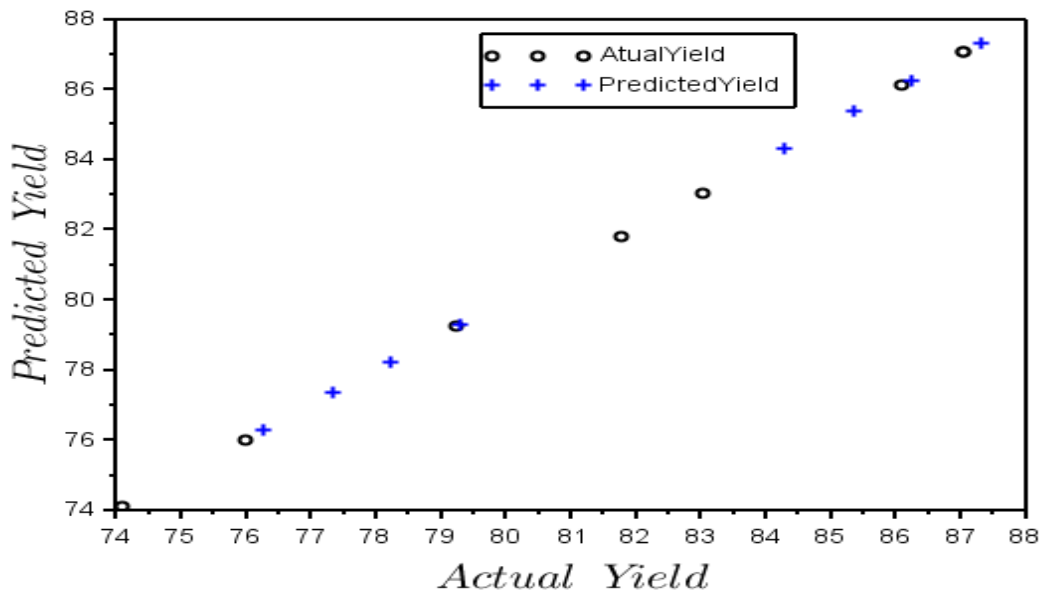


Figure 4-1: Correlation plot (Actual yield vs. Predicted yield)

Second order quadratic polynomial models approximated to singularity under the same experimental conditions. Below are surface plots showing biodiesel yield at variation of control parameters. Keeping time constant at t=60 min, whilst varying stirring rate and reaction temperature yields what is observed in figure 4.2 and 4.3.

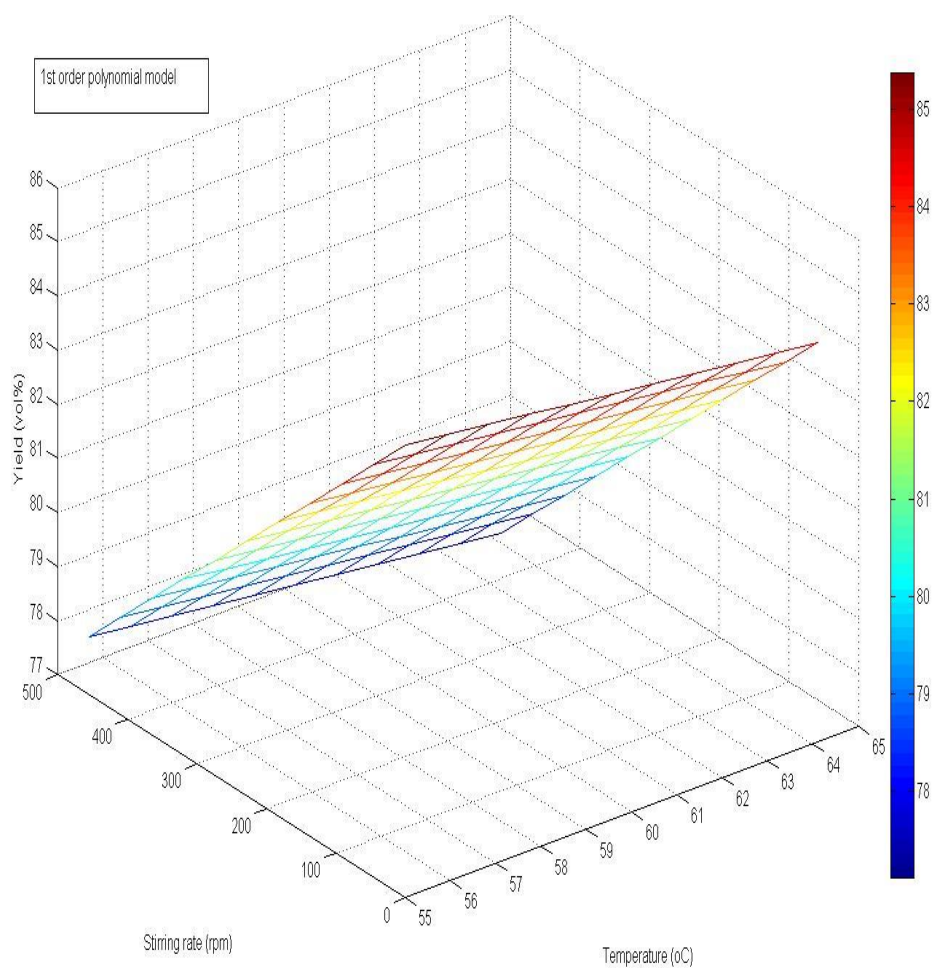


Figure 4-2: Response surface plot for the production of *Jatropha curcas* methyl esters at varying conditions (Methanol to Oil molar ratio 6:1, KOH catalyst 1%w/w oil)

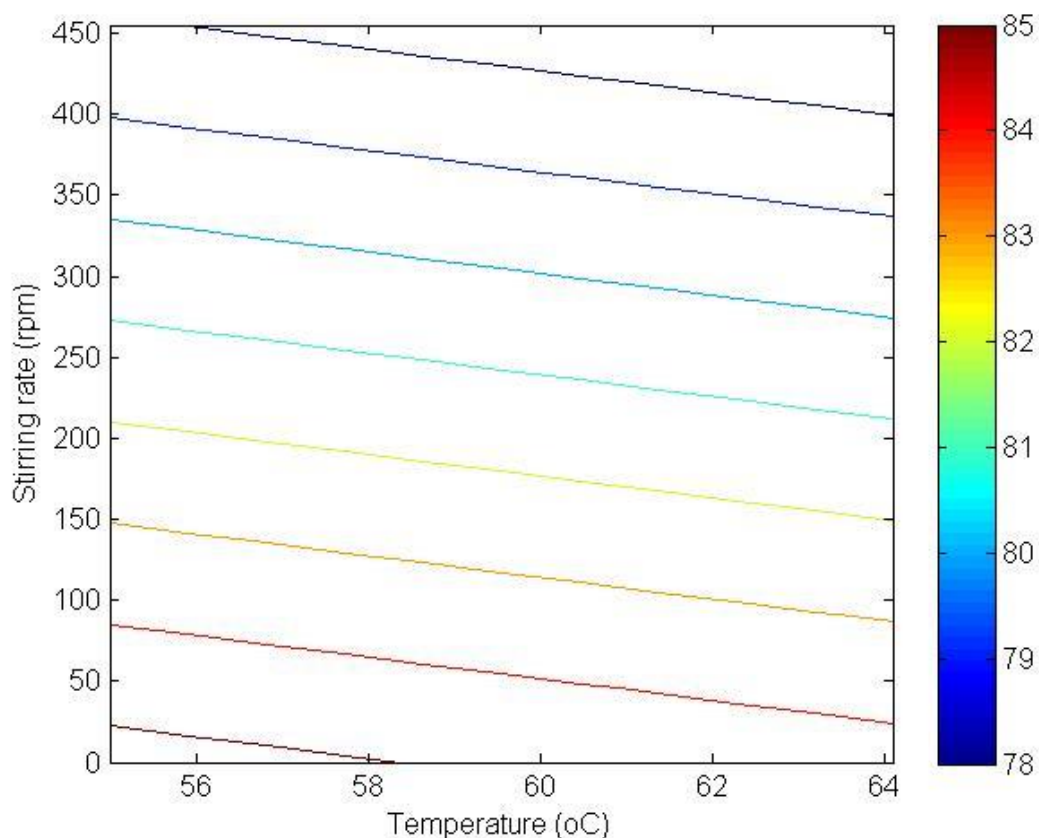


Figure 4-3: Contour plot for the production of *Jatropha curcas* methyl esters at varying conditions (Methanol to Oil molar ratio 6:1, KOH catalyst 1%w/w oil)

As shown from the graphs above, the response surface plots adequately describe the behavior of parameters as observed from experimentation. The rate constants are functions of temperature, and the highest yields (>85%) are obtained from the temperature range of approximately 55 °C with agitation speed of 0-250 rpm to aid the reaction. These results do not agree with those found in Okullo *et al.* (2010); in the sense that under similar experimental conditions, the polynomial regression equation obtained by Okullo *et al.* (2010) is a quadratic regression equation and surface plots depict a proportional relationship between biodiesel yield and agitation. Agitation is known to boost homogenization of a reaction and therefore results in higher biodiesel yields, however based on findings by Sharma and Singh (2007) the mode of stirring .i.e. mechanical or magnetic, also plays a role in the oil triglyceride conversion. In the study by Pedavoah (2010); it was found that the yield of biodiesel increased when a mechanical stirrer was used instead of a magnetic stirrer. A plausible explanation for this could be that the activity of the mechanical stirrer relatively increases the collision frequency of reagent molecules.

The unexpected behavior of stirring rate with respect to biodiesel can also be attributed to the number of experimental points used to develop the model. The first order design method used for this study is the 2^3 full factorial design, which took in 8 possible interactions, four of which are low coded (-1), and another four high coded (+1). This merely means that there are only 4 points that represent the response of biodiesel yield with higher agitation rates. In addition, the experiment was not previously designed for studying the influence of operating parameters, and therefore some results were omitted in this study due to the fact that they did not fit into any parameter interaction scenario required on the 2^3 full factorial design methodology. A maximum stirring rate of 250 rpm at a minimum 55 °C would result in biodiesel yields of above 81%. The optimum conditions for this experiment were found to be T=55 °C, molar ratio=6:1, catalyst concentration= 1% based on oil weight, and stirring rate of 0 to 250 rpm. While the optimum conditions found by Okullo *et al.* (2010) are T=55 °C, molar ratio=6:1, 1wt% catalyst concentration, and agitation speed of 600 rpm.

4.1.2 Kinetic model from literature

A theoretical model discussed in chapter 3 of this research report was used to fit concentration-time data of the transesterification of *Jatropha curcas* oil obtained from Mu'azu *et al.* (2015). The transesterification of *Jatropha curcas* seed oil was performed at three different temperatures (45 °C, 50 °C, and 55 °C), with methanol to oil molar ratio of 10:1, and agitation speed of 700rpm under heterogeneous catalysis (8 wt% calcium oxide, CaO). Figure 4.4 represents the experimental results for the transesterification of *Jatropha Curcas* oil at the temperature of T=45 °C. The initial estimation of k-values was obtained by using the three-point method (slopes at instant time) (Seoud & Abdallah, 2010). Thereafter the 4th order Runge-Kutta method was utilised to solve the system of ordinary differential equations. The least square regression analysis technique was performed with Scilab© software, Ver. 5.5.2 (2015), in order to find optimised k-values.

The experimental data in Figures 4.4, 4.6, and 4.8 was used to obtain the initial estimation of the k-values using the three point method; thereafter the theoretical model derived in Chapter 3 was solved by means of the 4th order Runge-Kutta whilst simultaneously optimizing the rate constant values thus giving rise to the closest fit as depicted by Figures 4.5, 4.7, and 4.9 respectively.

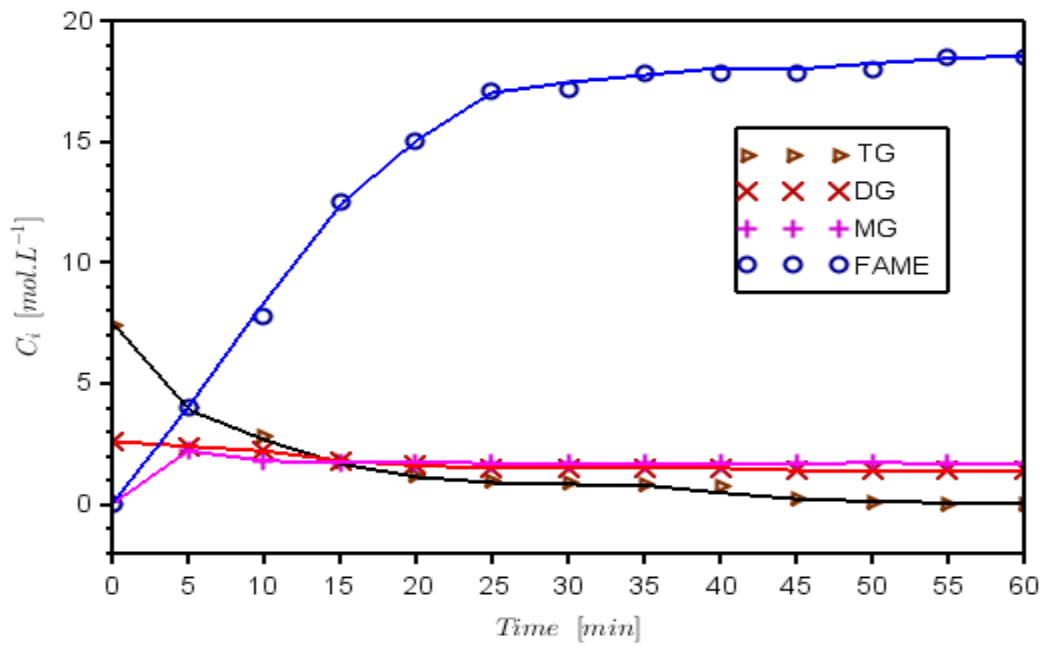


Figure 4-4: Experimental concentration-time data of Jatropha Curcas oil transesterification at T=45°C (Mu'azu, *et al.*, 2015)

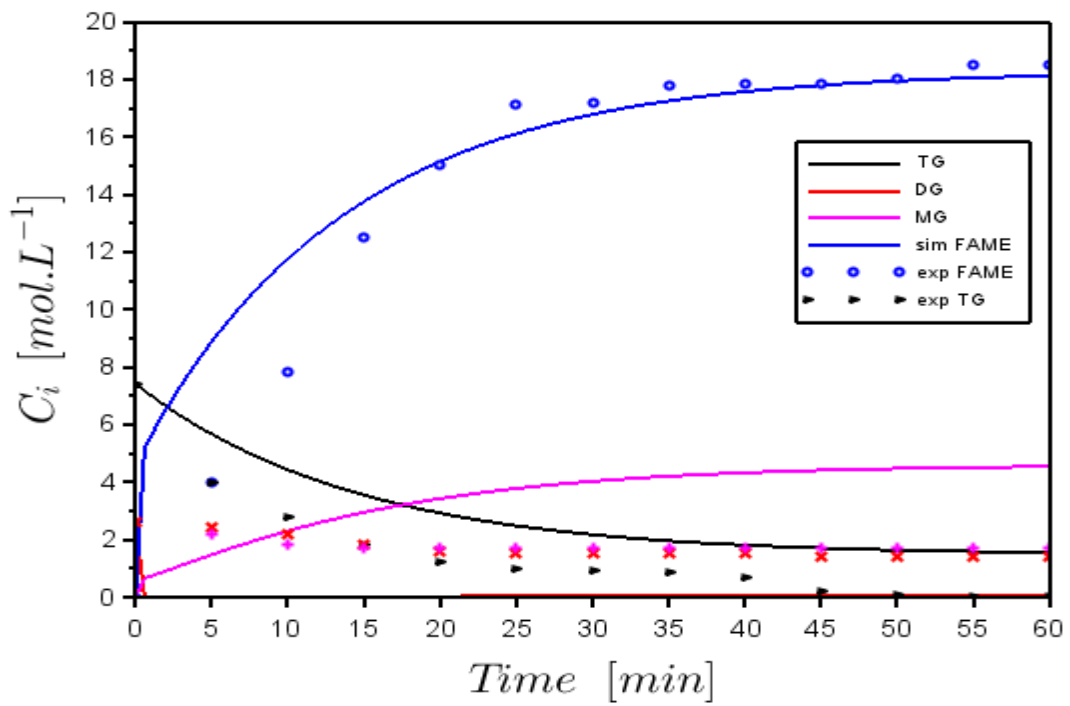


Figure 4-5: Scilab Simulated model at T=45°C

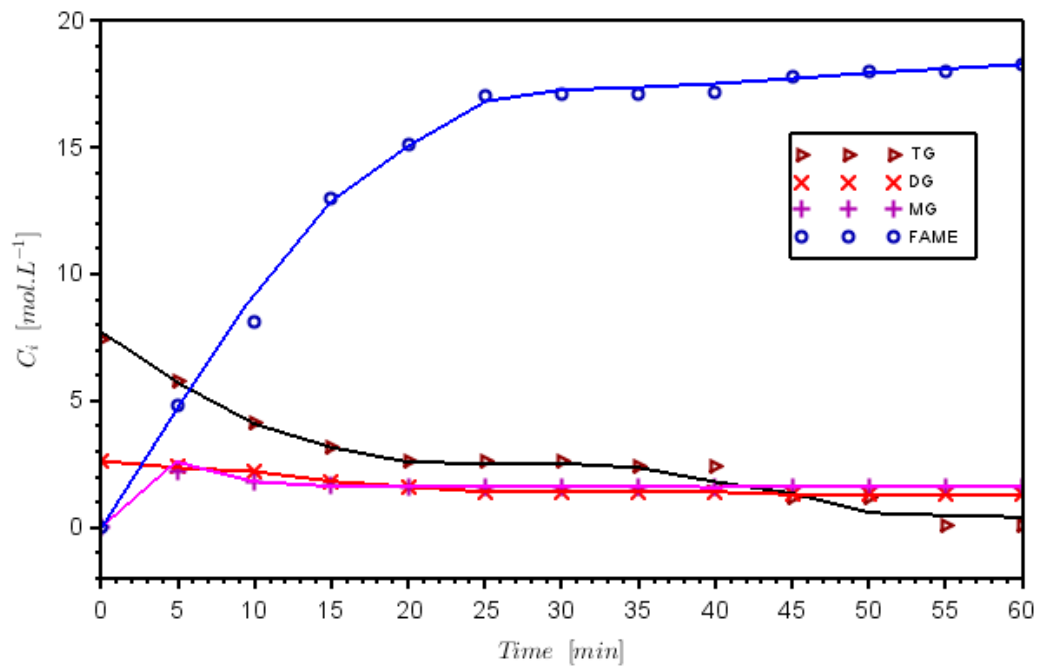


Figure 4-6: Experimental concentration-time data *Jatropa curcas* oil transesterification at T=50°C (Mu'azu, *et al.*, 2015)

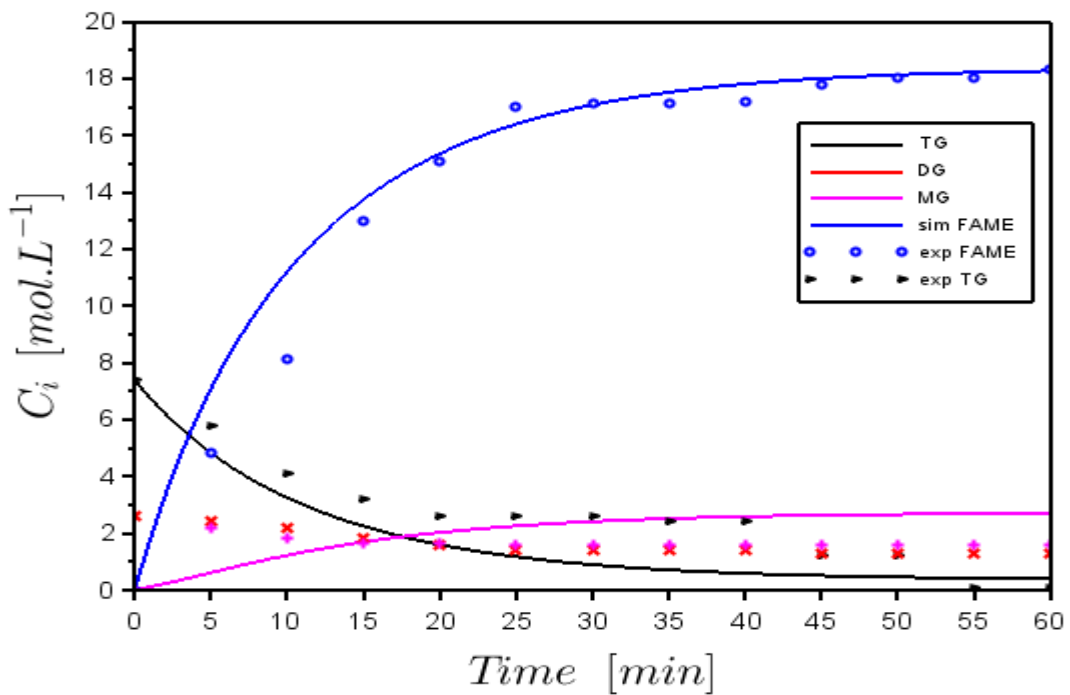


Figure 4-7: Scilab Simulated model at T=50°C

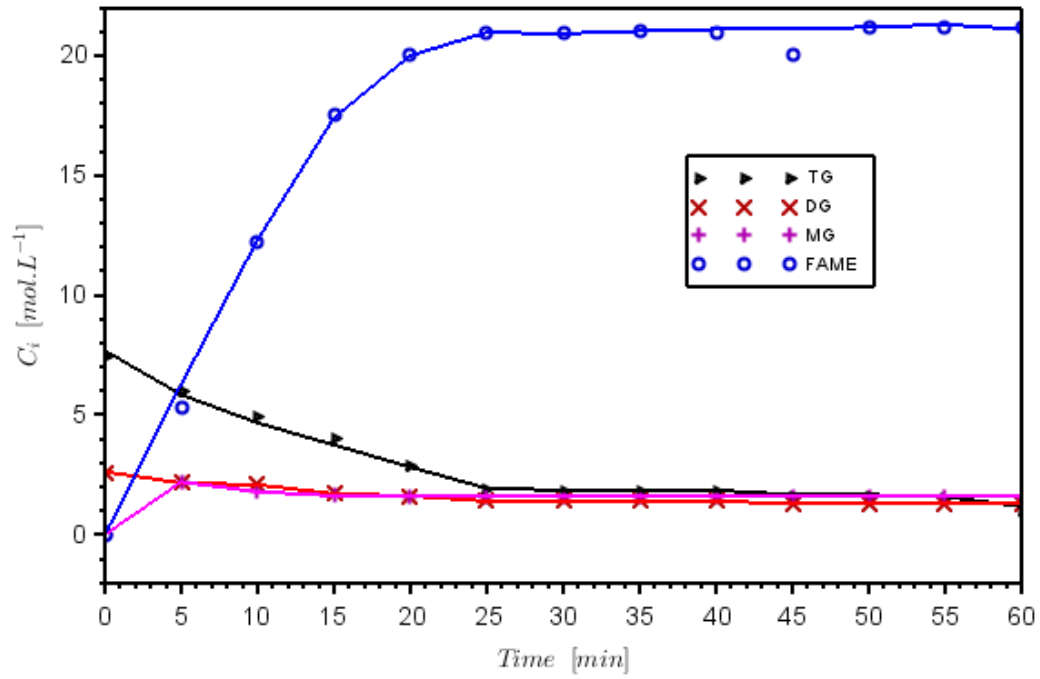


Figure 4-8: Experimental concentration-time data *Jatropa curcas* oil transesterification at T=55°C (Mu'azu, *et al.*, 2015)

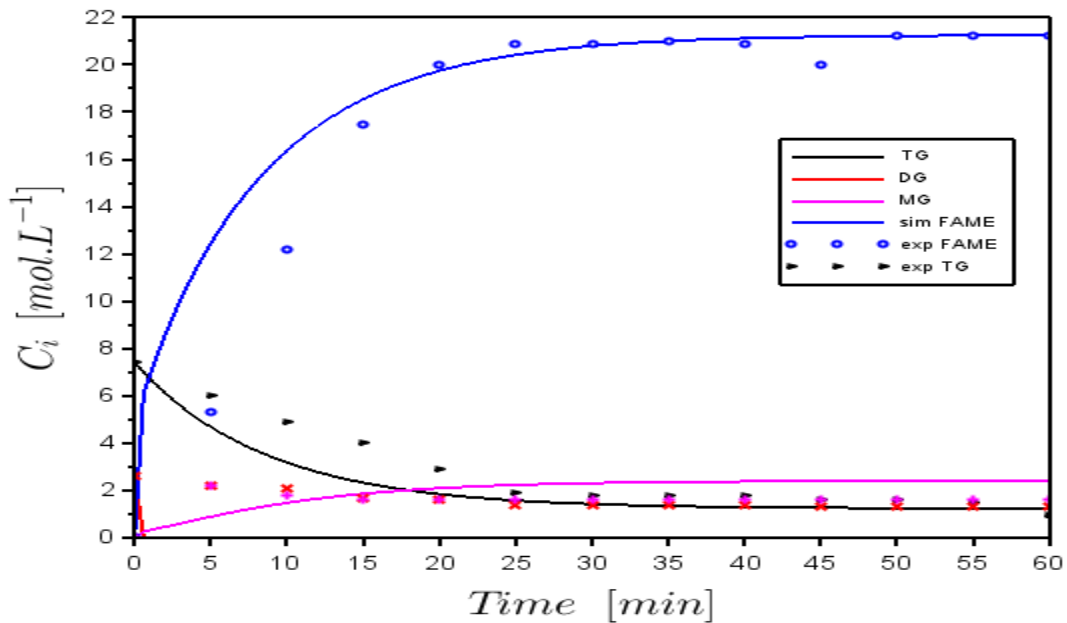


Figure 4-9: Scilab simulated model at T=55°C

The reaction proceeds rapidly from 0-25 minutes then stabilizes. After 25 minutes no significant changes in concentration of components were observed. For temperature of 55°C a significant change in concentration of components is in the range of 0- 20 min, this confirms the assumption made earlier in chapter 3 that the rate constants are only temperature dependent. There are two possible reasons why there is insignificant concentration change after 25 minutes, one is that the reactions have reached equilibrium, and the second reason is that as the reaction proceeds a glycerol rich-phase is formed and the catalyst is transferred into the glycerol phase, therefore decreasing the catalyst concentration consequently decreasing the rate of reaction (Mu'azu, *et al.*, 2015). Table 4.4 gives the rate constants that were obtained for transesterification of *Jatropha curcas* oil at all three temperatures. Better correlation was observed for reactions conducted at 55°C. The rate constant for the conversion of TG at different temperatures is relatively smaller than other rate constants for forward reactions, this means that the conversion of TG to form DG is slower and therefore the rate determining step. The rate constants for the production of MG are relatively high, which is why the simulated model shows that there is no significant conversion of MG to DG and hence the diglycerides decrease almost to completion whilst there is a remainder of monoglycerides after the reaction has stopped.

Table 4-4: Rate kinetics at different temperatures

Reaction	Rate constant (L/mol/min)	Temperature (°C)		
		45	50	55
TG→DG	k1	0.0006	0.0009	0.0011
DG→TG	k2	0.1	0.1	0.55
DG→MG	k3	0.21703372	0.4016	0.73704
MG→DG	k4	0.00836637	0.00933	0.01037
MG→G	k5	0.1	0.3	0.4
G→MG	k6	0.53043663	0.52671	0.56291

➤ **Determining activation energy and pre-exponential factor**

Obtained k-values are plotted against absolute temperature in order to estimate the Arrhenius pre-exponential factor and the minimum activation energy required for the reaction of the rate determining step to occur. The activation energy and pre-exponent factor for the rate

determining step is computed with the use of Arrhenius equation, in which E_a/RT is the slope of the plot and $\ln(k_0)$ is the intercept.

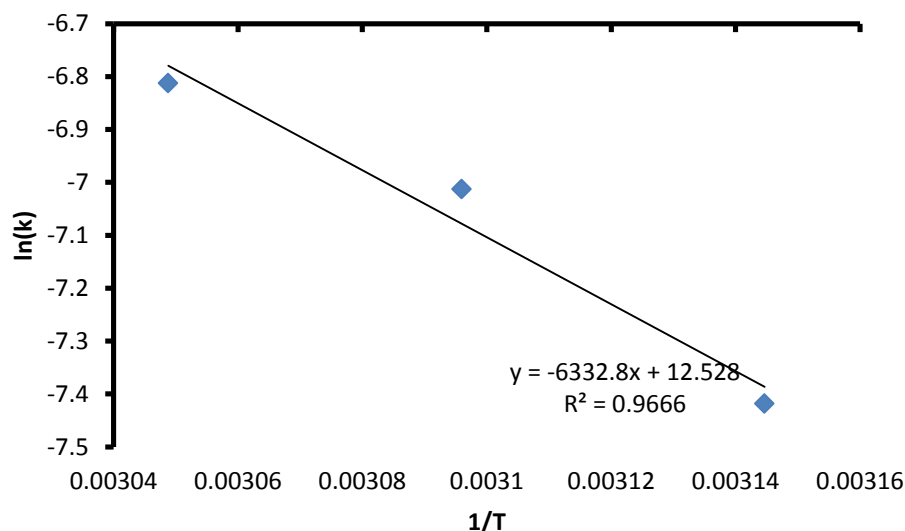


Figure 4-10: Determining activation energy and pre-exponential factor

The pre-exponential factor is found to be 275956.9/min and the minimum activation energy required for TG conversion is 52650.9 J/mol.

4.1.3 Empirical model

Theoretical model discussed above is based on the rate law of the observed behavior of the reaction mechanism. These generally give a good indication of model behavior without taking into account other possible reaction mechanisms governed by the same rate law. Given the number of theoretically possible interactions it would be better to attempt to derive a model that considered also other reaction mechanisms, which is why good assumptions and knowledge of reaction kinetics for a particular reaction mechanism is crucial. Knowledge of reaction kinetics and rate of reaction is determined through experimentation (Pedavoah, 2010).

For the theoretical model the reaction order was assumed, however in order to correctly identify or estimate reaction order of reacting components, a graph relating concentration and time is plotted. For the given experimental conditions the alcohol is fed in excess at a the methanol to oil ratio of 10:1, with this knowledge the rate of reaction is derived from an

irreversible overall reaction (equation 4-2) of TG to biodiesel and it is assumed that the rate of change of alcohol is negligible with respect to the rate of change of TG.



The rate of reaction for equation (4-3) with n^{th} overall reaction order is

$$\frac{dC_{TG}}{dt} = kC_{TG}^n \quad (4-3)$$

Concentration-time data for transesterification of *Jatropha curcas* was fitted in Figures 4.11-4.22 in order to determine the order of reaction. Table 4.5 gives a summary of optimized rate constants and correlation coefficients for first and second order kinetics at different temperatures. From the results obtained it is evident that the transesterification of *Jatropha curcas* is first order with respect to TG. First order kinetics show an overall better fit as evidenced by the high correlation coefficients. Freedman *et al.* (1986) declared that there is a condition called pseudo-first order that occurs when the concentration of alcohol is assumed constant due to the very high molar ratio of alcohol to the TG. The concentration of alcohol is fed in excess in this experiment which would explain the pseudo first order behaviour

Table 4-5: Verification of order of reaction

		T (°C)				Ea (kJ/mol)	
		45		50		55	
Order	Rate Constants	R ²	Rate Constants	R ²	Rate Constants	R ²	
1st order	0.041	0.8728	0.055	0.7038	0.094	0.865	71.838
2nd order	0.010045	0.8742	0.0125	0.4616	0.033	0.4918	301.432

➤ **Fitting 1st order kinetics model**

Figure 4.11 shows the simulated model for the 1st order kinetics at 45°C using equation (4-7), the model exhibits a similar behavior to that of experimental data especially in the first 15 minutes of the reaction. Figure 4.12 depicts the correlation coefficients of the data to model. The correlation coefficient is 0.872, which ascertains that a 1st order kinetic

model is a good fit with minimal error. The derivation of the first order kinetic model is as follows:

$$\frac{dC_{DG}}{dt} = -kC_{TG} \quad (4-4)$$

Integrating the rate equation yields equation (4-5)

$$\ln C_{TG} = -kt + C \quad (4-5)$$

$$\ln C_{TG} = -kt + \ln C_{TGO} \quad (4-6)$$

Substituting the Arrhenius equation results in equation (4-7)

$$\ln C_{TG} = -\left(k_0 e^{\frac{-E_a}{RT}}\right)t + \ln C_{TGO} \quad (4-7)$$

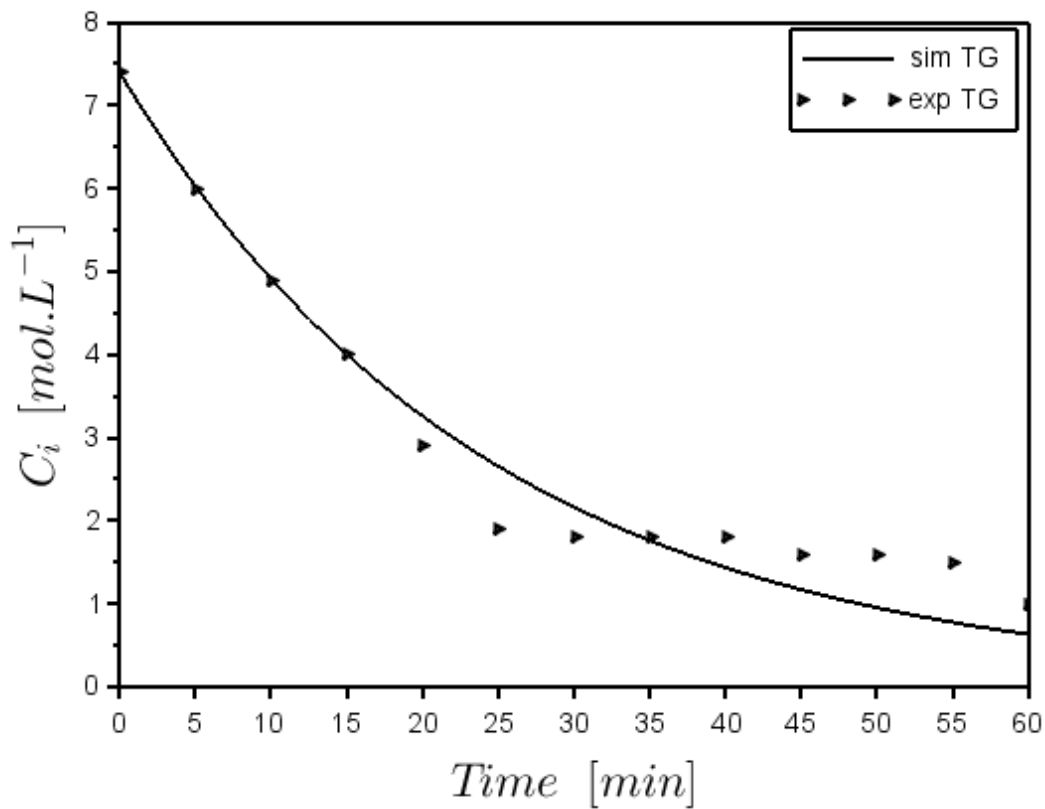


Figure 4-11: Variation of TG with time assuming first order kinetics at T=45°C, k=0.041/L

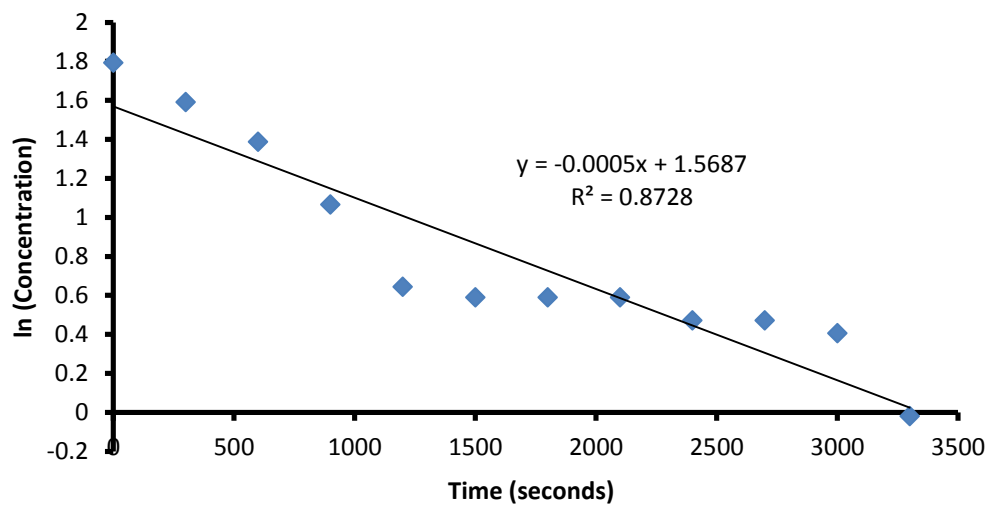


Figure 4-12: Verification of first order kinetics at T=45°C

Running the experiment at 50°C shows a lower correlation to 1st order kinetics compared to a minimum temperature of 45°C. The reaction shows a better relation with first order kinetics in the first 20 minutes and thereafter deviates, although not significantly. The correlation coefficient is 0.7038, verifying that the reaction does follow first order kinetics.

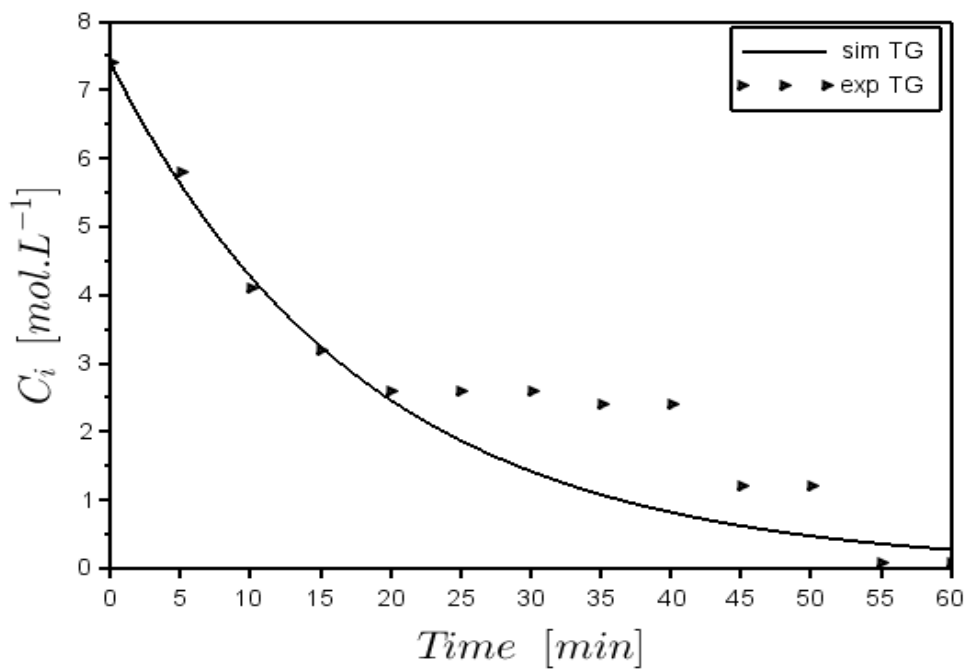


Figure 4-13: Variation of TG with time assuming first order kinetics at T=50°C, k=0.055/L

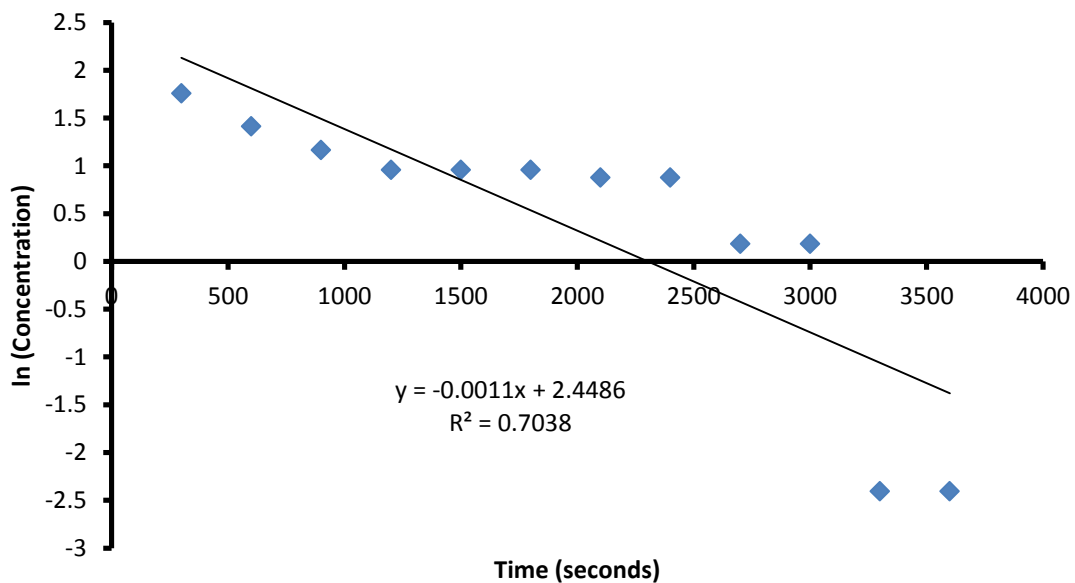


Figure 4-14: Verification of first order kinetics at T=50°C

From Figures 4.15 and 4.16, it can be seen that at 55°C the modelled reaction follows first order kinetics, which has significantly lower deviations from experimental data. The correlation coefficient is 0.865. The observation from this is that the reaction exhibits first order kinetics behaviour more at the temperatures of 45°C and 55°C.

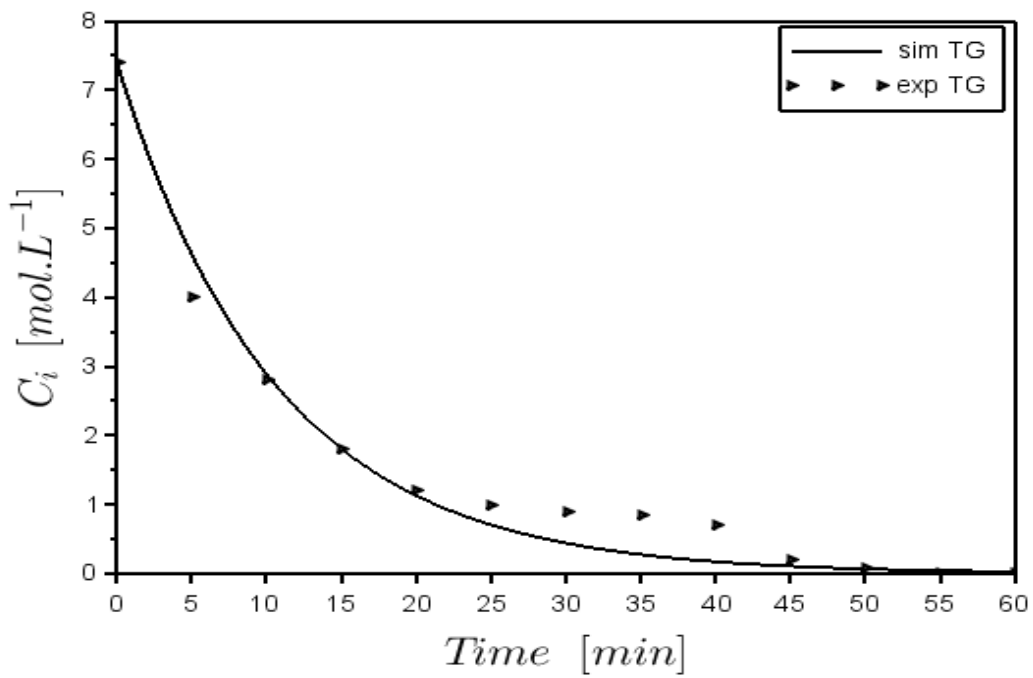


Figure 4-15: Variation of TG with time assuming first order kinetics at T=55°C, k=0.094/L

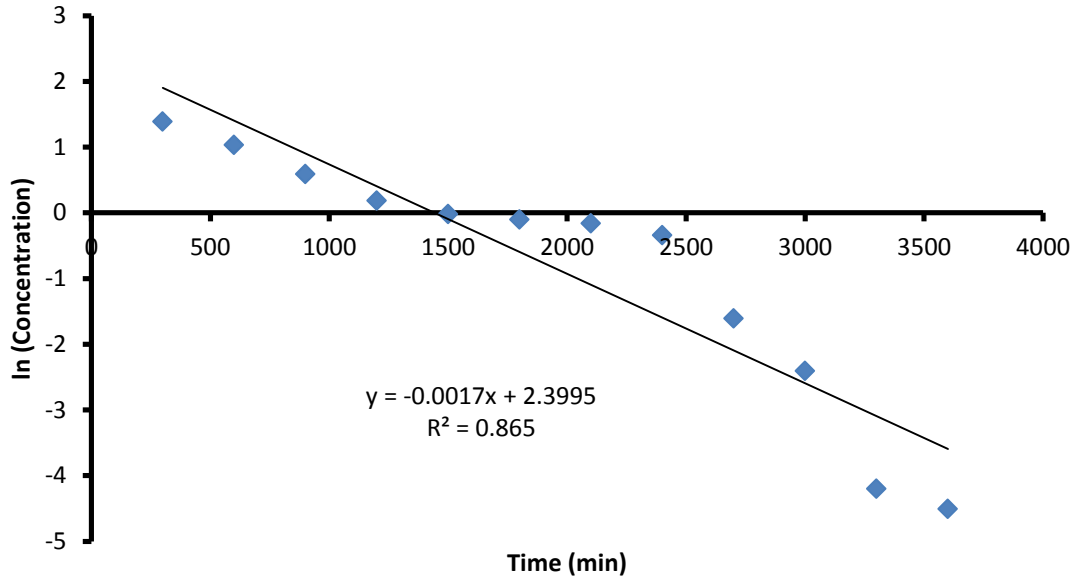


Figure 4-16: Verification of first order kinetics at T=55°C

It is important to explore the possibility of the reaction following second order reaction kinetics. Figures 4.17 to 4.23 show how the experimental data compares to a second order kinetic model at different temperatures. The derivation of the second order kinetic model is shown through equation (4-8) to equation (4-10). At 45°C the reaction displays a second order behaviour after 40 minutes accompanied by a high correlation coefficient. As the temperatures increase to 50 °C and 60 °C, the reaction displays less of the 2nd order kinetics.

➤ **Fitting 2nd order kinetics model**

$$\frac{dC_{TG}}{dt} = -kC_{TG}^2 \quad (4-8)$$

$$\frac{1}{C_{TG}} = kt + C \quad (4-9)$$

$$\frac{1}{C_{TG}} = \left(k_0 e^{\frac{-E_a}{RT}} \right) t + \frac{1}{C_{TGO}} \quad (4-10)$$

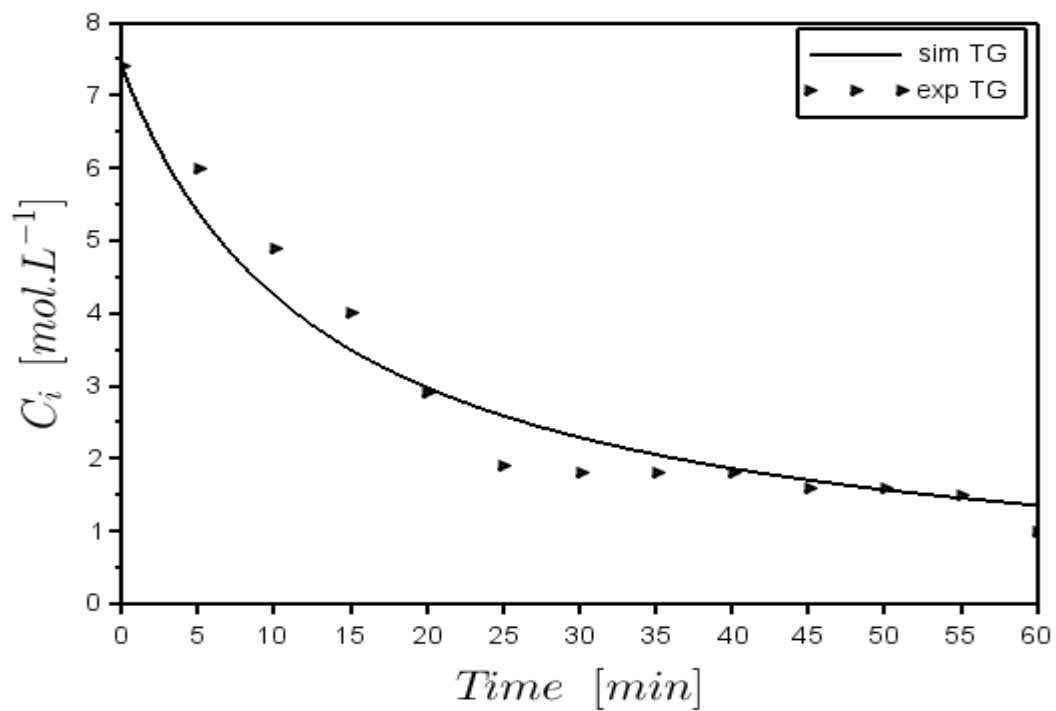


Figure 4-17: Variation of TG with time assuming second order kinetics at $T=45^{\circ}\text{C}$, $k=0.010045\text{ L/mol/min}$

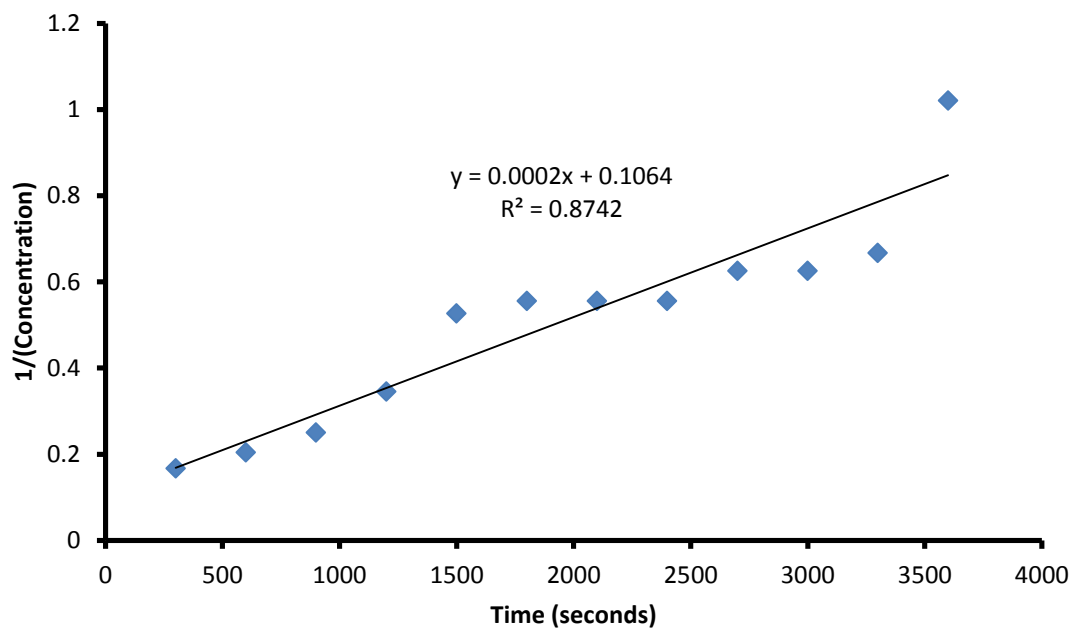


Figure 4-18: Verification of second order kinetics, $T=45^{\circ}\text{C}$

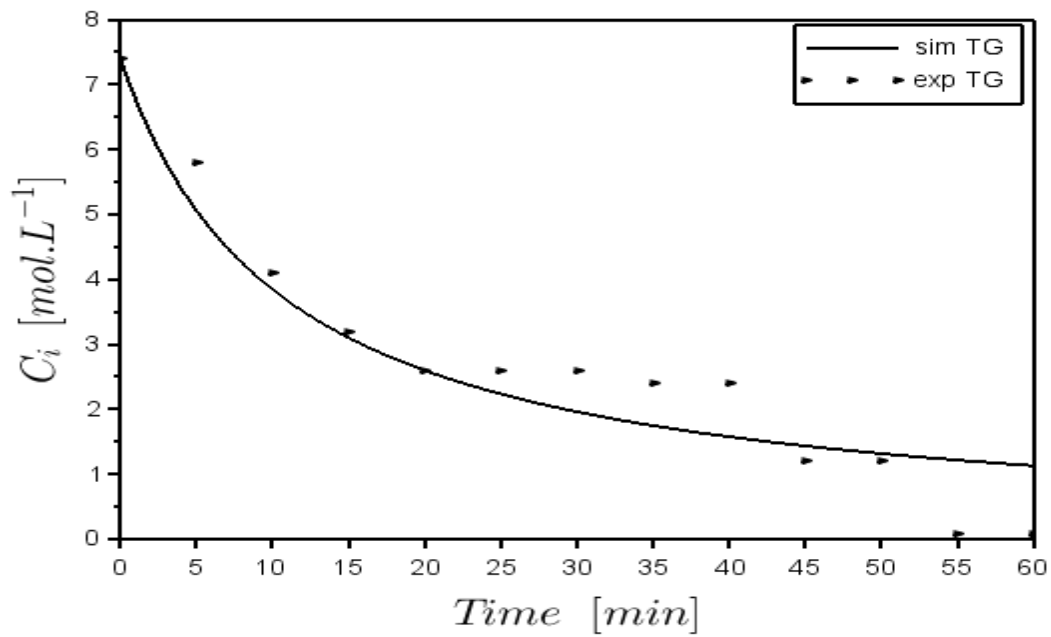


Figure 4-19: Variation of TG with time assuming second order kinetics at T=50°C, k=0.0125L/mol/min

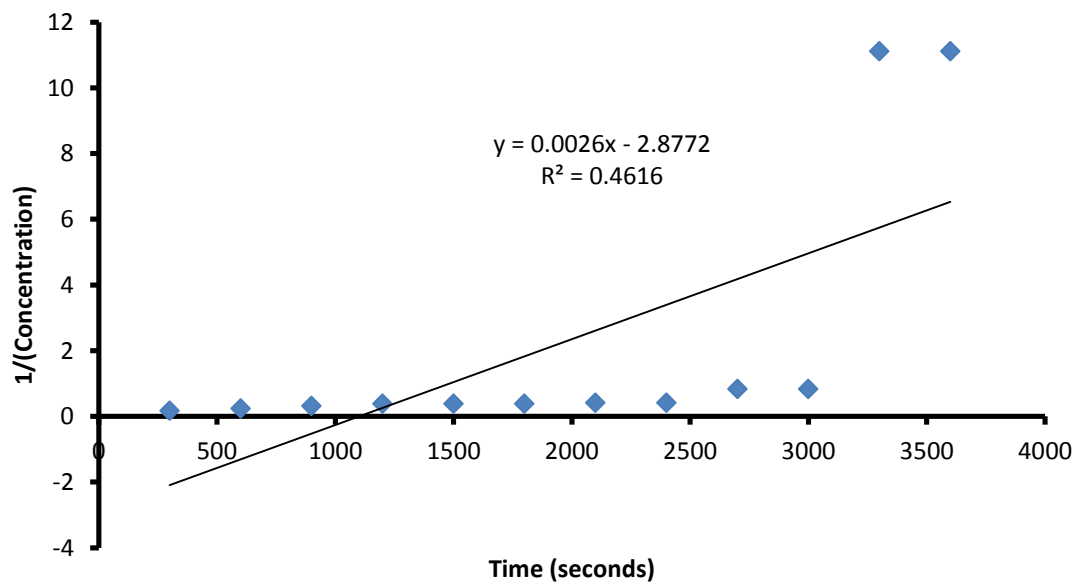


Figure 4-20: Verification of second order kinetics at T=50°C

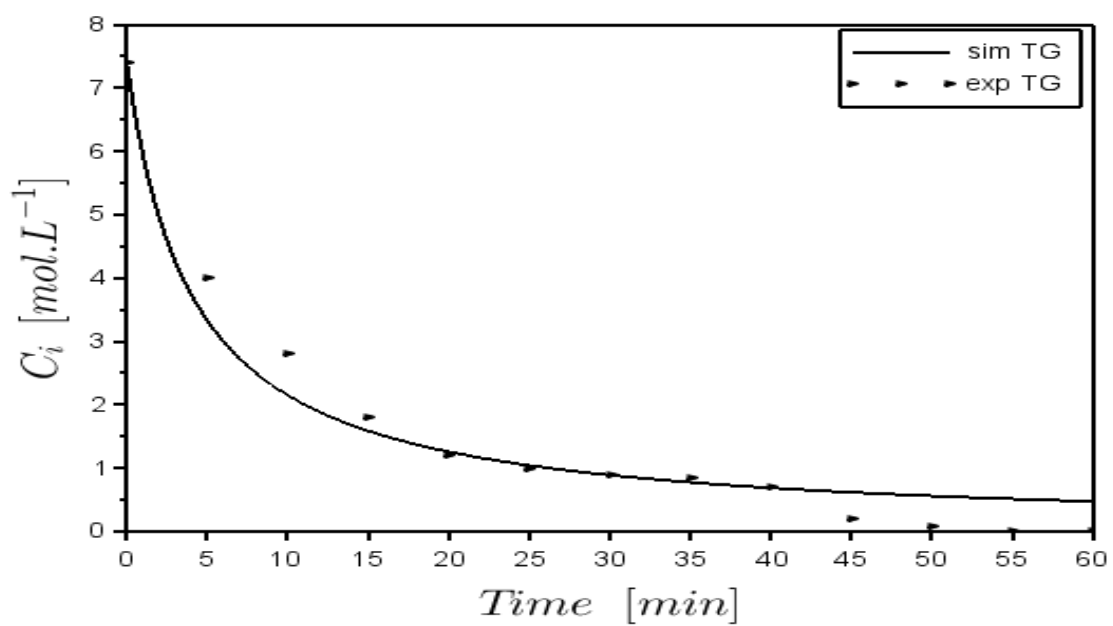


Figure 4-21: Variation of TG with time assuming second order kinetics at $T=55^{\circ}\text{C}$, $k=0.033\text{ L/mol/min}$

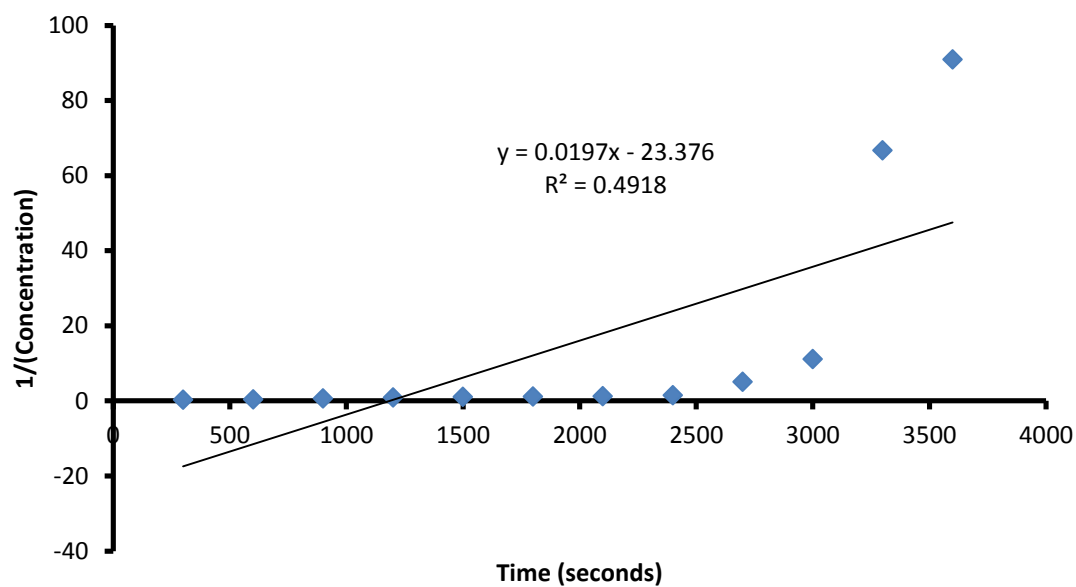


Figure 4-22: Verification of second order kinetics at $T=55^{\circ}\text{C}$

➤ Determining activation energy and pre-exponential factor

First order kinetics

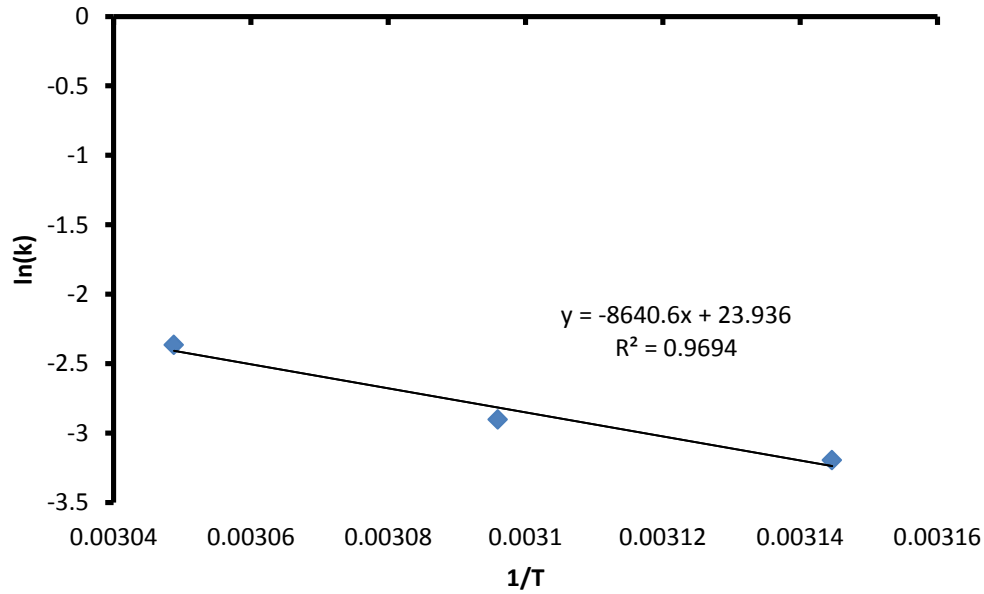


Figure 4-23: Activation energy and pre-exponential factor (First order kinetics)

The value of the pre-exponential factor is $2.48 \times 10^{10} / \text{min}$ and the minimum activation energy required for the reaction to take place is 71837.95 J/mol. Therefore the rate equation for the transesterification of Jatropha curcas seed oil using Calcium Oxide (CaO) as heterogeneous catalyst is given by (Equation 4-12).

$$\frac{dC_{TG}}{dt} = \left(k_0 e^{\frac{-E_a}{RT}} \right) C_{TG}^1 \quad (4-11)$$

$$\frac{dC_{TG}}{dt} = \left(2.48e10 * e^{\frac{-71837.95}{8.314*T}} \right) C_{TG}^1 \quad (4-12)$$

Second order kinetics

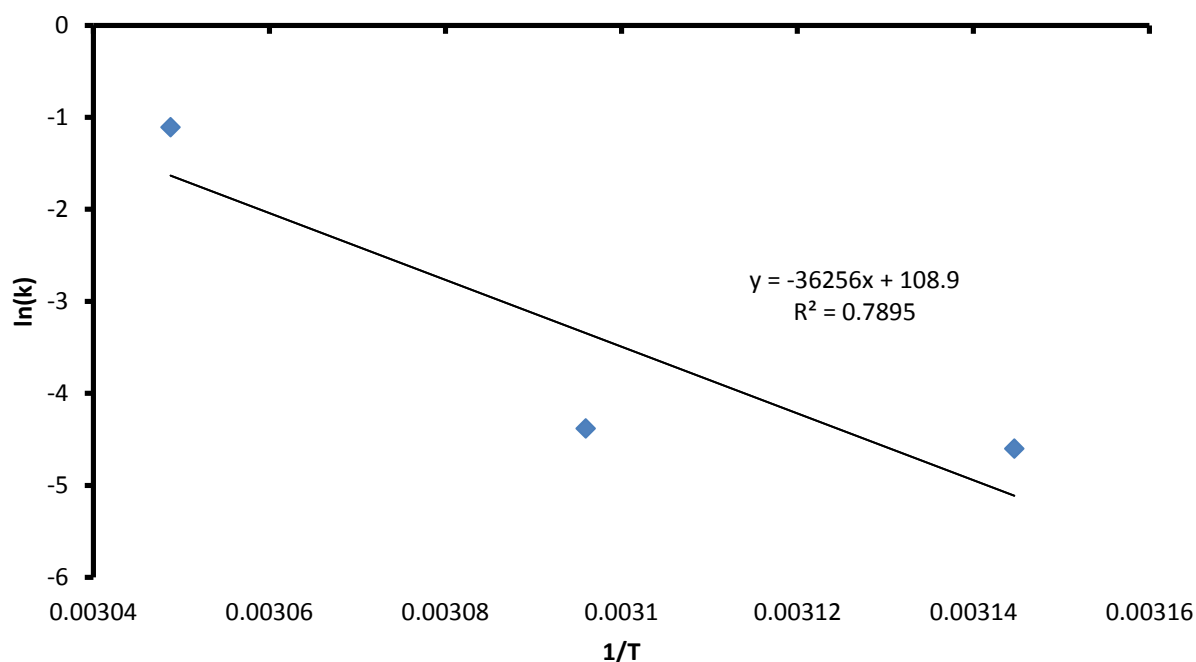


Figure 4-24: Activation energy and pre-exponential factor

The value of the minimum activation energy required for the reaction to take place is 301432 J/mol and the pre-exponential factor is 1.97092×10^{47} . The rate equation is given by (equation 4-14);

$$\frac{dC_{TG}}{dt} = -kC_{TG}^2 \quad (4-13)$$

$$\frac{dC_{TG}}{dt} = -(1.97e47 e^{\frac{-301432}{(8.3140T)}})C_{TG}^2 \quad (4-14)$$

4.1.4 Model validation

In section 4.1.2 a theoretical kinetic model was used to fit experimental data for Jatropha curcas oil transesterification under heterogeneous catalysis. The order of reaction was assumed to be first order with respect to reacting components. In section 4.1.3 the order of reaction was verified by curve fitting of the concentration-time data, with the knowledge that alcohol is fed in excess and therefore its rate is insignificant.

To verify the order of reaction, alternative data from Ude *et al.* (2016) and Veljkovic *et al.* (2006) were fitted to the first order reaction model. The former is for the transesterification of jatropha curcas with 0.6w% KOH catalyst and the latter for the transesterification of tobacco seed oil (Nicotiana tabacum L.) with two step process due to its high content of free fatty acids .The two-step process serves as pre-treatment of high FFA oil by employing acid catalysis, called esterification and thereafter transesterification using KOH catalyst for biodiesel yield. This study mainly focuses on low FFA oil; hence the results from based catalysed transesterification were used for kinetic analysis. It is important to note that as opposed to experimental conditions discussed in section 4.1.2, the experimental data for model validation was obtained from experiments performed under homogeneous catalysis. The purpose of using alternative data obtained from different conditions was to study the general behaviour of non-edible oils transesterification.

Jatropha curcas TG transesterification generally follows the first order reaction behaviour, as can be seen from figures 4.25 to 4.33. It is fascinating to note however that at a temperature of 60°C the reaction shows better correlation for a second order reaction, the same is observed for transesterification of tobacco seed oil.

(a) Tobacco Seed oil

The experimental conditions for Tobacco seed oil are found in appendix B:

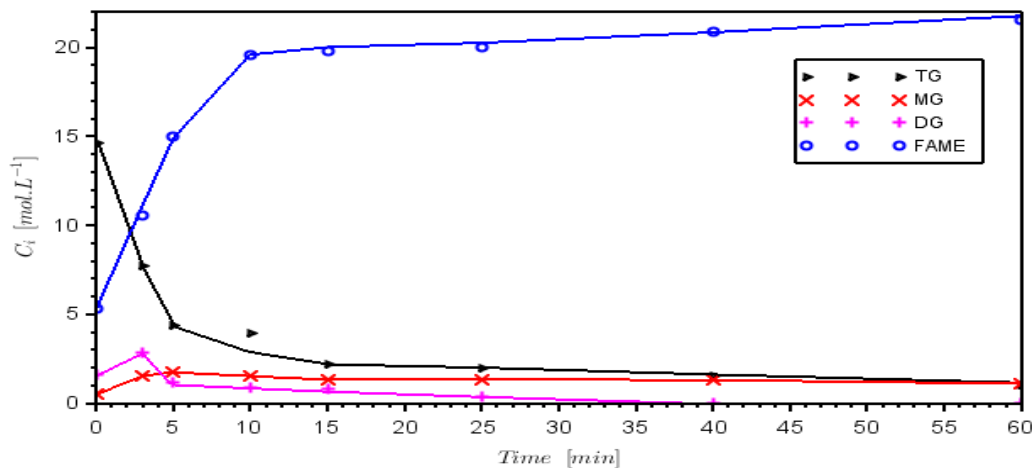


Figure 4-25: Experimental concentration-time data, T=60°C (Veljkovic', *et al.*, 2006)

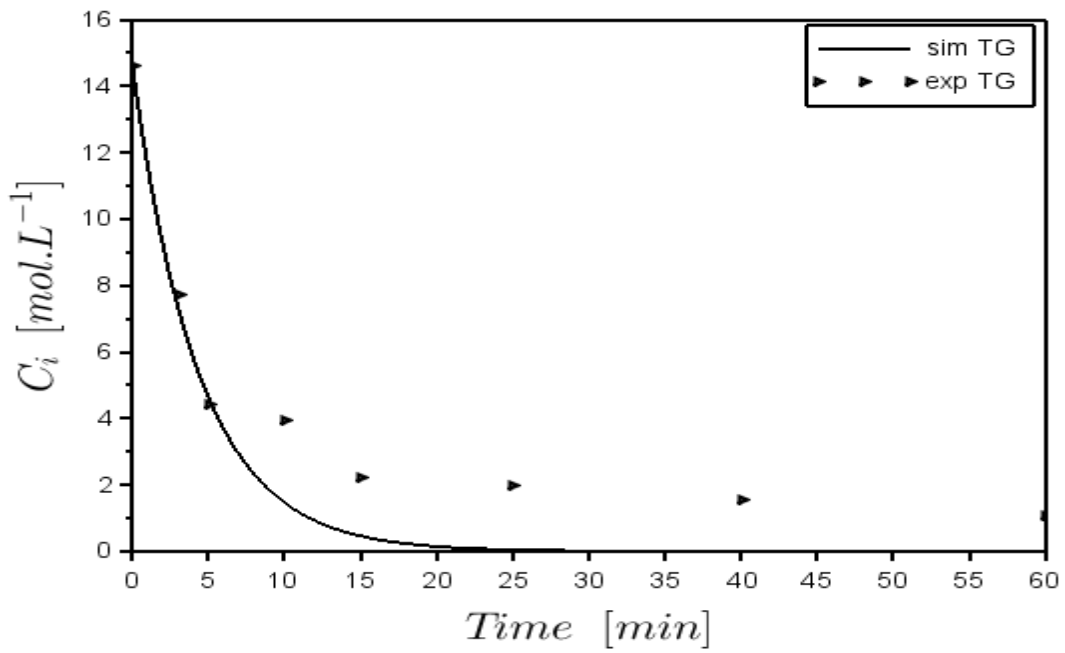


Figure 4-26: Simulated results of the variation of TG with time assuming first order kinetics at $T=60^{\circ}\text{C}$, $k=0.23/\text{L}$

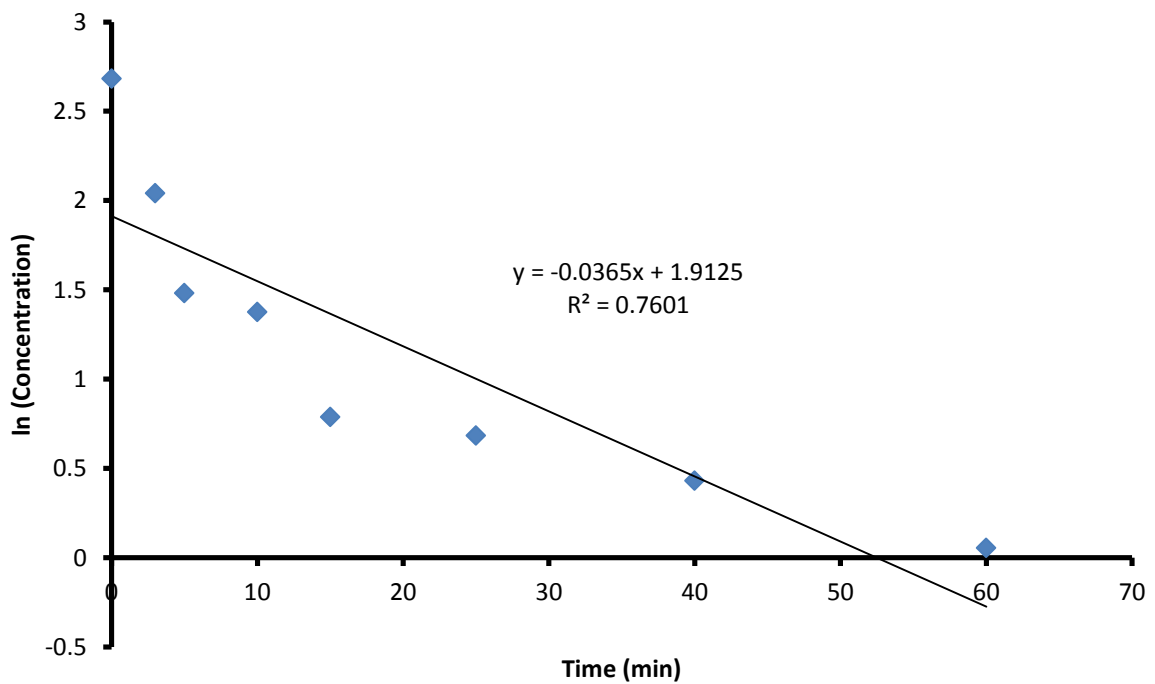


Figure 4-27: verification of first order kinetics, $T=60^{\circ}\text{C}$

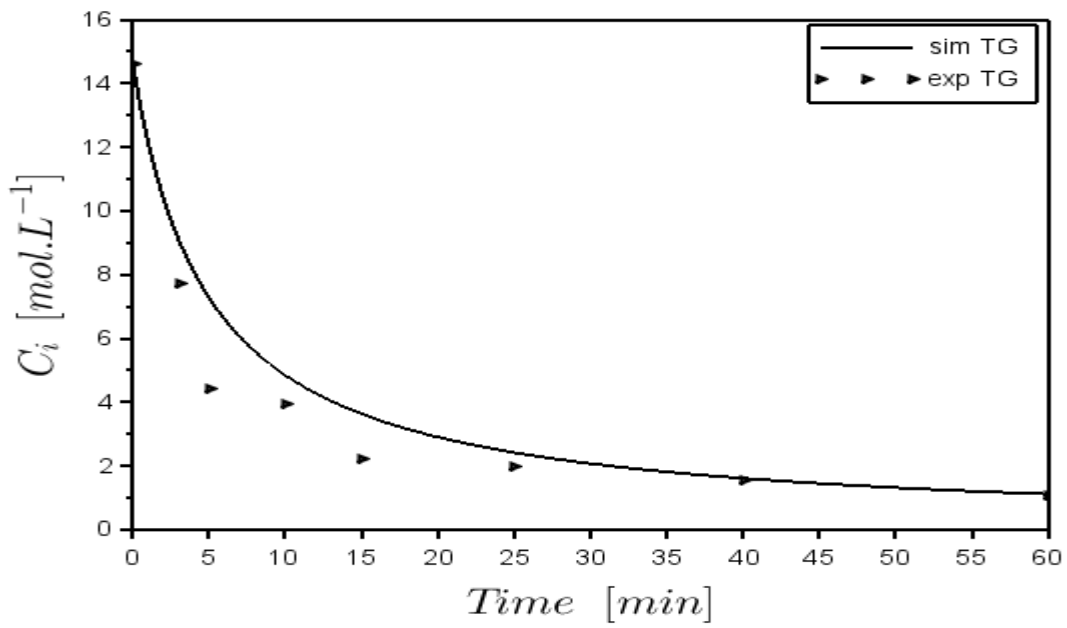


Figure 4-28: Simulated results for the variation of TG with time assuming second order kinetics at $T=60^{\circ}\text{C}$, $k=0.0138\text{L/mol/min}$

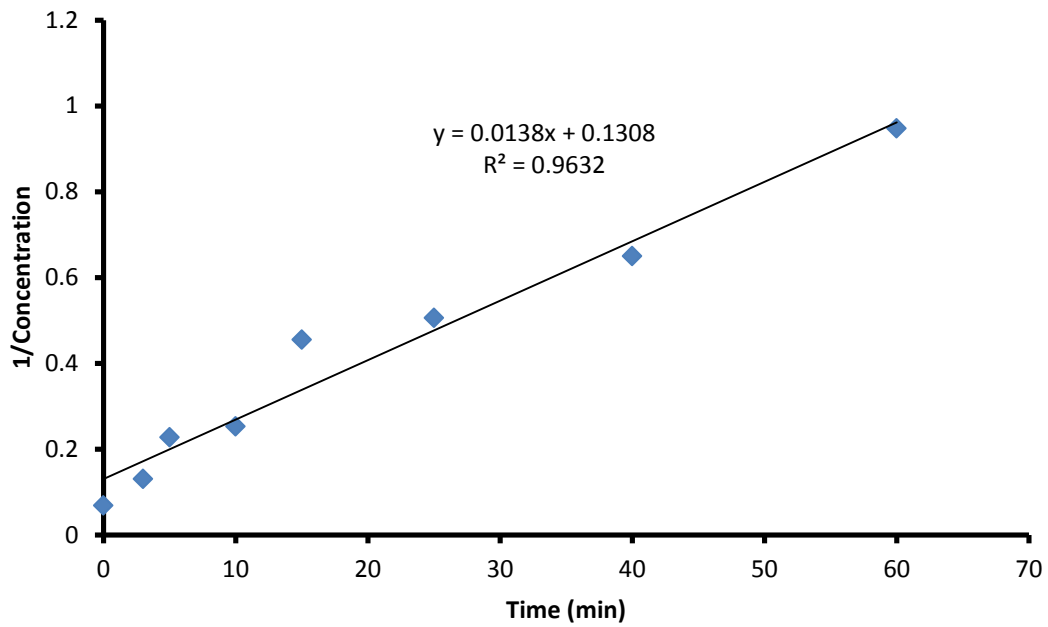


Figure 4-29: Verification of second order kinetics, $T=60^{\circ}\text{C}$

(b) Jatropha Curcas oil

First order verification (Ude, *et al.*, 2016)

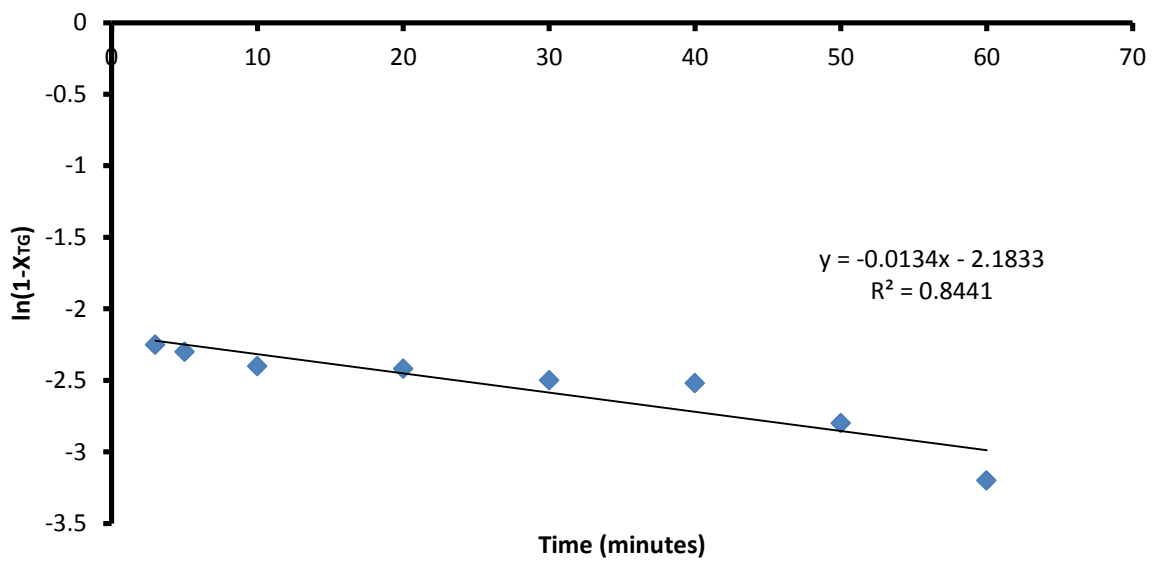


Figure 4-30: Verification of first order kinetics at T=50°C

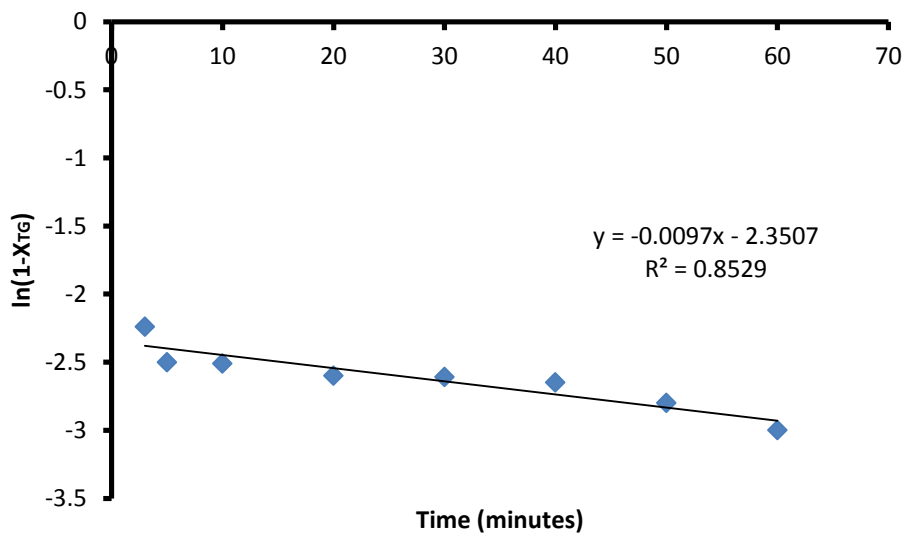


Figure 4-31: Verification of first order kinetics at T=60°C

Second order kinetics verification

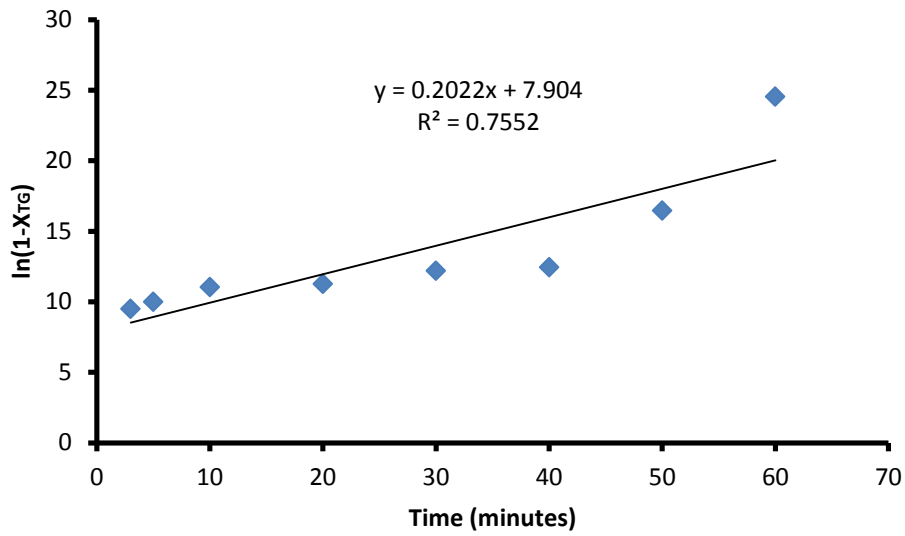


Figure 4-32: Verification of second order kinetics at T=50 °C

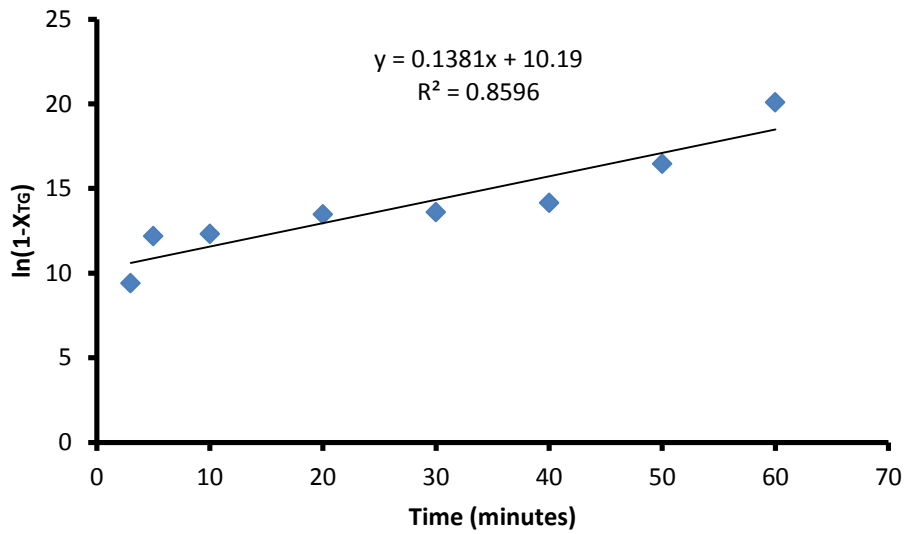


Figure 4-33: Verification of second order kinetics at T=60°C

CHAPTER 5

5. Conclusion

The kinetics study of transesterification of biodiesel from non-edible oils (jatropha curcas oil and tobacco seed oil) was carried out. The effects of temperature, molar ratio, agitation speed and reaction time were studied with the aid of response surface plots in order to understand the influence of these operating parameters during the production of biodiesel. It was found that temperature does increase the rate constant of a reaction and therefore leads to higher biodiesel yields. The optimum temperature was found to be 55°C, and the highest biodiesel yields are found at this temperature when no agitation is involved. The order of reaction with respect to oil triglycerides was found to be first order at temperatures from 45°C to 55°C; however at temperatures above 60°C the correlation was higher for second order kinetics. This was observed in both tobacco seed oil and jatropha curcas seed oil transesterification under homogeneous catalysis. It is concluded therefore that at optimum temperatures of 55°C the transesterification of oil triglyceride (for both heterogeneous and homogeneous catalysis) is first order. Based on these findings it can be stated that the kinetic behaviour of non-edible oils is similar and can be explained by a general pseudo first order kinetic model given by (equation 4-7) when alcohol is fed in excess at temperatures of approximately 55°C. For temperatures above 60°C the reaction is second order with respect to oil triglycerides and can be modeled using (equation 4-10). Assuming order of reaction from theory is accurate under similar conditions as those studied in theory but given the complexities of chemical kinetics it is best to verify unknown parameters from experimental data obtained. With these findings it is evident that no one kinetic model can be globalised for the transesterification of all non-edible oils.

CHAPTER 6

6. Recommendations

A good design of experiments is beneficial in predicting the behaviour of control parameters such as temperature, catalyst concentration etc. therefore it is recommended that any attempt to perform an experiment on the transesterification of oil for biodiesel synthesis should be preceded by a good design of experiments and thereafter a robust response surface methodology. This is to ensure that the experiments are conducted only at optimum conditions. When modelling the kinetic behaviour of the reactions, experimental data should be used first to verify reaction orders and other unknown parameters, and parameter value obtained from literature should only be used as a base or initial guess. The orders of reaction are independent of temperature and therefore only change as the reaction changes. A further investigation would be to determine how a reaction changes at high temperatures resulting in second order kinetics. It would be beneficial to also explore if in fact most non-edible oils behave this way and at what combination of control parameters. With South Africa currently exploring jet biofuel, further investigations on the transesterification kinetics of Tobacco seed oil as well as response surface methodology would prove beneficial so as to confirm the behaviour observed above.

7. References

- Anastopoulos, G., Zannikou, Y., Stournas, S. & Kalligeros, S., 2009. Transesterification of Vegetable Oils with Ethanol and Characterization of the Key Fuel Properties of Ethyl Esters. *energies*, Volume 2, pp. 362-376.
- Ugbogu, A. E. et al., 2013. Nutritional and chemical composition of *Jatropha curcas* (L) seed oil. *International Journal of Biosciences*, 3(6), pp. 15-25.
- Veljkovic', V., Lakićević', S. & Stamenko, O., 2006. Biodiesel production from tobacco (*Nicotiana tabacum* L.) seed oil with a high content of free fatty acids. *Fuel*, pp. 2672-2676.
- ASTM, 2005. *ASTM Standards Related to Biodiesel Fuel Blend Stock (B100) for Middle Distillate Fuels*, s.l.: ASTM.
- Balat, M., 2011. Potential alternatives to edible oils for biodiesel production- A review. *Energy Covers Manage*, pp. 1479-1492.
- Bankovic-Ilic, I. B., Stamenkovic, O. S. & Veljkovic, V. B., 2012. Biodiesel production from non-edible plant oils. *Elsevier: Renewable and Sustainable Energy Reviews*, pp. 3621-3647.
- Barnwal, B. & Sharma, M., 2005. Prospects of biodiesel production from vegetable oils in India. *Renew Sustain Energy Rev*, pp. 363-378.
- Berchmans, H. & Hirata, S., 2008. Biodiesel production from crude *Jatropha curcas* L. seed oil with a high content of free fatty acids. *Bioresour Technol*, pp. 1716-1721.
- Bikou, E., Louloudi, A. & Papayannakos, N., 1999. The effect of water on the transesterification kinetics of cotton seed oil with ethanol. *Chemical Engineering & Technology*, pp. 70-75.
- Botte, J.-M., 2016. *The future of automotive and fuels for a sustainable development*. Johannesburg, Total Professeurs Associés, p. 30.
- Bournay, L., 2005. New heterogenous process for biodiesel production: A way to improve the quality and the value of the crude glycerin produced by biodiesel plants. *Catal Today*, pp. 190-192.

- Brown, R., 2003. *Biorenewable Resources*. Iowa: Blackwell Publishing Co..
- Casey, T., 2015. *Cleantechnica*. [Online]
Available at: <https://cleantechnica.com/2015/09/02/tobacco-aviation-biofuel-ready-takeoff-25-years-rd/>
[Accessed 4 March 2017].
- Cavalcante, K., Penha, M., Mendonça, K. & Louzeiro, H., 2010. Optimization of transesterification of castor oil with ethanol using central composite rotatable design (CCRD). *Fuel*, pp. 1172-1176.
- Chitra, P., Venkatachalam, P. & Sampathrajan, A., 2005. Optimisation of experimental conditions for biodiesel production from alkali-catalysed transesterification of *Jatropha curcus* oil. *Energy Sustain Dev*, pp. 8-13.
- da Silva, N., Batistella, C., Filho, R. & Maciel, M., 2009. Biodiesel production from castor oil: optimisation of alkaline ethanolysis. *Energy Fuels*, pp. 5636-5642.
- Deng , X., Fang, Z. & Liu, Y., 2010. Ultrasonic transesterification of *Jatropha curcus* L oil to biodiesel by a two step process. *Energy Covers Manage*, pp. 2802-2807.
- Encinar, J., Gonzalez, J. & Rodriguez-Reinares, A., 2005. Biodiesel from used frying oil: Variables affecting the yields and characteristics of the biodiesel. pp. 5491-5499.
- ESI Africa, 2016. Africa's Power Journal. *Biofuel makes history in South Africa*, 20 July, p. 1.
- Freedman, B., Butterfield , R. & Pryde, E., 1986. Transesterification kinetics of soybean oil. *JAACS*, pp. 1375-1380.
- Ghadge, S. & Raheman, H., 2005. Biodiesel production from mahua (*madhuca indica*) oil having high FFAs. *Biomass Bioenergy*, pp. 601-605.
- Gui, M., Lee, K. & Bhatia, S., 2008. Feasibility of edible oil vs non edible oil as biodiesel feedstock. *Energy*, pp. 1646-1653.
- He, H., Sun, S. & Wang, T., 2007. Transesterification kinetics of soybean oil for production of biodiesel in supercritical methanol. *JAACS*, pp. 399-404.
- Helwan, Z. et al., 2009. Technologies for production of biodiesel focusing on green catalytic techniques: A reiew. *Fuel Process Technol*, pp. 1502-1514.

- Jain, S. & Sharma, M., 2010. Prospect of biodiesel from *Jatropha* in India: A review. *Renew Sustain Energy Rev*, pp. 763-771.
- Janaun, J. & Ellis, N., 2010. Perspectives on biodiesel as a sustainable fuel. *Renew Sustain Energy Rev*, pp. 1312-1320.
- Jaun, J., Kartika, D., Wub, T. & Hin, T., 2011. Biodiesel production from *Jatropha* oil by catalytic and non-catalytic approaches: An overview. *Bioresour Technol*, pp. 452-460.
- Karmakar, A., Karmakar, S. & Mukherjee, S., 2010. Properties of various plants and animal feedstocks for biodiesel production. *Bioresour Technol*, pp. 7201-7210.
- Kavrakis, S. & Wood, L., 2009. *Biodiesel Production from Jatropha curcas Oil*, WORCESTER: WORCESTER POLYTECHNIC INSTITUTE.
- Koh, M. & Ghazi, T., 2011. A review of biodiesel production from *Jatropha curcas* L oil. *Renew Sustain Energy Rev*, pp. 4732-4745.
- Komers, K., 2002. Kinetics and mechanism of the KOH-catalyzed methanolysis of rapeseed oil for biodiesel production. *Eur Lipid Sci*, pp. 728-737.
- Kralova, I. & Sjöblom, J., 2010. Biofuels-Renewable energy sources: A review. *J Dispers Sci Technol*, pp. 409-425.
- Kumar, A. & Sharma, S., 2011. Potential non-edible oil resources as biodiesel feedstock: An Indian perspective. *Renew Sustain Energy Rev*, pp. 1999-2008.
- Kumar, S., Chaubea, A. & Jain, S., 2012. Sustainability issues for promotion of *Jatropha* biodiesel in Indian Scenario: A review. *Renew Sustain Energy Rev*, pp. 1089-1098.
- Leung, D., Wu, X. & Leung, M., 2010. A review of biodiesel production using catalysed transesterification. *Appl Energy*, pp. 1083-1095.
- Liu, J., 2013. *Biodiesel synthesis via transesterification reaction in supercritical methanol: a) A kinetic study, b) Biodiesel synthesis using microalgae oil*, s.l.: Syracuse University.
- Lopez, D., Goodwin, J. & Bruce, D., 2007. Transesterification of Triacetin with Methanol on Nafion Acid Resins. *J Catal*, p. 379.
- Lotero, E., 2005. Synthesis of biodiesel via acid catalysis. *Ind Eng Chem Res*, pp. 5353-5363.

- Ma, F. & Hanna, M., 1999. Biodiesel Production: A review. *Bioresour Technol*, pp. 1-15.
- Meher, L., Vidya, S. & Naik, S., 2006. Technical aspects of biodiesel production by transesterification-A review. *Renewable Sustain Energy Rev*, pp. 248-268.
- Mittelbach, M., 1990. Transesterification of heated rapeseed oil for extending diesel fuel. *JAACS*, pp. 545-550.
- Mittelbach, M. & Remshmidt, C., 2006. *Biodiesel*. Graz, Austria, Martin Mittelbach.
- Mu'azu, K. et al., 2015. Kinetic Modeling of transesterification of Jatropha curcas seed oil using heterogeneous catalyst. *Engineering and Technology*, 2(3), pp. 87-94.
- Murugesan, A., Umarani, C., Chinnusamy, T. & Krishan, M., 2009. Production and analysis of biodiesel from non-edible oils- A review. *Renew Sustain Energy Rev*, pp. 825-834.
- Noureddini, H. & Zhu, D., 1997. Kinetics of transesterification of soybean oil. *J Am Oil Chem Soc*, pp. 1457-1463.
- Okullo, A. A. & Temu, A. K., 2015. Modelling the kinetics of Jatropha Oil for Transesterification. *Energy and Power Engineering*, Volume 7, pp. 135-143.
- Okullo, A., Temu, A., Ntalikwa, J. & Ogwok, P., 2010. Optimization of Biodiesel Production from Jatropha Oil. *International Journal of Engineeirng Research in Africa*, 3(62), pp. 62-73.
- Pedavoah, M. M., 2010. *Process optimization and the Kinetics of transesterification of Jatropha Curcas oil*, Kumasi: Kwame Nkrumah University of Science and Technology.
- Pramanik, K., 2003. Properties and use of Jatropha curcas oil and diesel fuel blends in compression ignition engine.. *Renewable Energy*, Volume 28, pp. 239-248.
- Saravanan, N., Puhon, S., Nagarajan, G. & Vedaraman, N., 2010. An experimental comparish of transesterification process with different alchls using acid catalysts. *Biomass Bioenerg*, pp. 999-1005.
- Seoud, A.-L. A. & Abdallah, L. A., 2010. Two Optimization Methods to Determine the Rate Constants of a Complex Chemical Reaction Using FORTRAN and MATLAB. *American Journal of Applied Sciences*, 7(4), pp. 509-517.

- Shahid, E. & Jamal, Y., 2010. Production of biodiesel: A technical Review. *Renew Sustain Energy Rev*, pp. 1312-1320.
- Sharma , Y. & Singh , B., 2007. . Development of biodiesel from karanja, a tree found in rural India. *J.Fuel*, 10(1016).
- Shika, K. & Rita, C., 2012. Biodiesel production fro non-edible oils: A review. *Renew Sustain Energy Rev*, pp. 1312-1320.
- Silitonga , A., Atabania, A. & Mahliaa, T., 2011. A review on prospect of Jatropha curcus for biodiesel in Indonesia. *Renew Sustain Energy Rev*, pp. 3733-3756.
- Sirisomboon, P., Kitchaiya, P. & Pholpho, T., 2007. Physical nd Mechanical properties of Jatropha curcas L fruits nuts and kernels. *Biosyst Eng*, pp. 201-207.
- Srinivas, K., Sudhakar babu, T., Raghavu rao, B. & Sivaragu, K., 2013. Experimental Analysis of Tobacco Seed Oil blends with diesel in single cylinderci-engineer. *International Journal of Engineering Trends and Technoloy (IJETT)*, 4(10), pp. 4535-4539.
- Tiwari, A. A. & Raheman, H., 2007. Biodiesel production from jatropha oil (Jatropha curcas) with high free fatty acids: An optimized process. *Biomass&BioEnergy*, pp. 569-575.
- Turner, T. L., 2005. *Modeling and Simulation of Reaction Kinetics for Biodiesel Production*, Raleigh: North Carolina State University.
- Ude, C. N., Onukwuli , D., Onwudiro, J. L. & Emembolu, . L. N., 2016. PREPARATION OF BODIESEL FROM NON-EDIBLE NIGERIAN JATROPHA CURCAS OIL: EFFECTS OF PROCESS PARAMETERS AND KINETICS OF REACTION. *Sigma Journal of Engineering and Natural Sciences*, Volume 3, pp. 415-437.
- Veljkovic´ , V. et al., 2006. Biodiesel production from tobacco (Nicotiana tabacum L.) seed oil with a high content of free fatty acids. *Fuel*, 04(15), pp. 2671-2675.
- Vyas, A., Verma, J. & Subrahmanyam, N., 2010. A review of FAME production processes. *Fuel*, pp. 1-9.
- Wang, R., Ham, M. & Zhou, W., 2011. Production and selected fuel properties of biodiesel from promising non-edible oils: Euphorbia Lsthyris L., Sapium Sebeferum L., and Jatropha curcus L.. *Bioresour Technol*, pp. 1194-1199.

Wang, Y., 2007. Preparation of biodiesel from waste cooking oil via two-step catalyzed process. *Energy Conversion and Management*, pp. 184-188.

Warabi, Y., Kusdiana, D. & Saka, S., 2004. Biodiesel fuel from vegetable oil by various supercritical alcohols. *Appl Biochem Biotechnol*, pp. 113-116, 793-801.

Yazdani, S. & Gonzalez, R., 2007. Anaerobic fermentation of glycerol: A path to economic viability for the biofuels industry. *Curr Opin Biotechnol*, pp. 213-219.

Appendices

APPENDIX A: Komers Model Derivation

APPENDIX B: Experimental Data Sheets

APPENDIX D: Simulation Codes

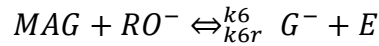
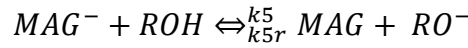
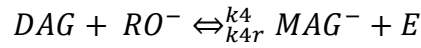
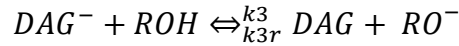
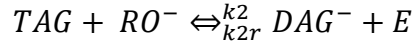
Appendix A: Komers Model Derivation

After applying the assumptions stated in section 2.6.2, the following possible reactions are obtained

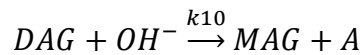
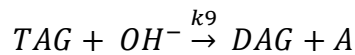
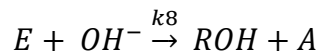
e) Formation of alkoxide:



f) Alcoholysis:



g) Saponification:



If the oil has high FFA content, the following equation needs to be considered,



It is assumed that the reactions above are elementary and therefore are governed by the law of mass action, which when applied gives thirteen differential equations involving thirteen species (Komers, 2002). To simplify the complexity of the differential equations, two common approaches can be chosen; one is that of the rate-limiting step assumption and the other is that of the steady state assumption (Turner, 2005). The rate limiting suggests that the rate of the conversion is controlled by the rate of slowest reaction, assuming that the fastest reactions have reached equilibrium. The steady state assumption states that some species react increasingly faster than others resulting in their rate of change being essentially zero (Turner, 2005). The approach taken by Komers is the steady state assumption as it gives rise to an algebraic equation with rate constants for all reacting species.

So assuming steady state, reactions 2, 4, and 6 of equation (A-2) proceed at much higher rate than the other reactions, thus

$$\begin{aligned}
 k_2, k_{2r} &\ll k_3, k_{3r} \\
 k_4, k_{4r} &\ll k_5, k_{5r} \\
 k_6, k_{6r} &\ll k_7, k_{7r} \\
 k_3, k_{3r}, k_5, k_{5r}, k_7, k_{7r} &> k_8, k_9, k_{10}, k_{11}
 \end{aligned} \tag{A-5}$$

Consequently, if the minor terms are removed and substituted into the rate equation at equilibrium conditions, the following is obtained

$$\frac{d[H_2O]}{dt} = \frac{d[RO^-]}{dt} = \frac{d[DAG^-]}{dt} = \frac{d[MAG^-]}{dt} = \frac{d[G^-]}{dt} = 0 \tag{A-6}$$

Using the initial concentrations of triacylglycerols $[TAG]_0$ and alcohol $[ROH]_0$ to normalise the remaining species, Komers obtained the following relations

$$\begin{aligned}
 TAG &= \frac{[TAG]}{a} \\
 DAG &= \frac{[MAG]}{a} \\
 G &= \frac{[G]}{a}
 \end{aligned}$$

$$\begin{aligned}
A &= \frac{[A]}{a} \\
OH &= \frac{[OH^-]}{a} \\
W &= \frac{[H_2O]}{a} \\
ROH &= \frac{[ROH]}{b} \\
E &= \frac{[E]}{b}
\end{aligned} \tag{A-7}$$

Where $a = [TAG]_0$ and $b = [ROH]_0$

Thus giving rise to the following differential equations:

$$-\frac{dTAG}{dt} = b \cdot OH \cdot (k'_2 \cdot TAG \cdot ROH - k'_{2r} \cdot DAG \cdot E) + a \cdot OH \cdot k_9 \cdot TAG$$

$$\begin{aligned}
-\frac{dDAG}{dt} &= b \cdot OH \cdot (-k'_2 \cdot TAG \cdot ROH + k'_{2r} \cdot DAG \cdot E + k'_4 \cdot DAG \cdot ROH - k'_{4r} \cdot MAG \cdot \\
&E) + a \cdot OH \cdot (-k_9 \cdot TAG + k_{10} \cdot DAG)
\end{aligned}$$

$$\begin{aligned}
-\frac{dMAG}{dt} &= b \cdot OH \cdot (-k'_4 \cdot DAG \cdot ROH + k'_{4r} \cdot MAG \cdot E + k'_6 \cdot MAG \cdot ROH - k'_{6r} \cdot G \cdot E) + \\
&a \cdot OH \cdot (-k_{10} \cdot DAG + k_{11} \cdot MAG)
\end{aligned}$$

$$\frac{dG}{dt} = b \cdot OH \cdot (k'_6 \cdot MAG \cdot ROH - k'_{6r} \cdot G \cdot E) + a \cdot OH \cdot k_{11} \cdot MAG$$

$$\begin{aligned}
-\frac{dROH}{dt} = \frac{dE}{dt} &= b \cdot OH \cdot (k'_2 \cdot TAG \cdot ROH - k'_{2r} \cdot DAG \cdot E + k'_4 \cdot DAG \cdot ROH - k'_{4r} \cdot MAG \cdot \\
&E + k'_6 \cdot MAG \cdot ROH - k'_{6r} \cdot G \cdot E - k_8 \cdot E)
\end{aligned}$$

$$-\frac{dOH}{dt} = \frac{dA}{dt} = b \cdot OH \cdot k_8 \cdot E + a \cdot OH \cdot (k_9 \cdot TAG + k_{10} \cdot DAG + k_{11} \cdot MAG)$$

$$-\frac{dH_2O}{dt} = \frac{dFFA}{dt} = a \cdot k_{12} \cdot FFA \cdot OH \quad (A-8)$$

Where,

$$\begin{aligned} k'_2 &= \frac{k_2 K_1}{W} \\ k'_{2r} &= \frac{k_{2r} K_1}{K_3 W} \\ k'_4 &= \frac{k_4 K_1}{W} \\ k'_{4r} &= \frac{k_{4r} K_1}{K_5 W} \\ k'_6 &= \frac{k_6 K_1}{W} \\ k'_{6r} &= \frac{k_{6r} K_1}{K_7 W} \end{aligned} \quad (A-9)$$

And

$$\begin{aligned} K_1 &= \frac{k_1}{k_{1r}} = \frac{[RO^-][H_2O]}{[ROH][OH^-]} \\ K_3 &= \frac{k_3}{k_{3r}} = \frac{[DAG][RO^-]}{[DAG^-][ROH]} \\ K_5 &= \frac{k_5}{k_{5r}} = \frac{[MAG][RO^-]}{[MAG^-][ROH]} \\ K_7 &= \frac{k_7}{k_{7r}} = \frac{[G][RO^-]}{[G^-][ROH]} \end{aligned} \quad (A-10)$$

The rate of reactions are represented by the following four balance equations

$$TAG + DAG + MAG + G = 1$$

$$ROH + E + 1$$

$$OH + A + p$$

$$\text{Where } p = \frac{[OH^-]_0}{[TAG]_0}$$

$$nE + 3TAG + 2DAG + MAG + A = 3 \quad (\text{A-11})$$

$$\text{Where } n = \frac{[ROH]_0}{[TAG]_0}$$

The initial conditions are given as

$$[TG]_0 = 1$$

$$[ROH]_0 = 1$$

$$[OH]_0 = p$$

$$[DG]_0 = [MG]_0 = [G]_0 = [E]_0 = [A]_0 = 0 \quad (\text{A-12})$$

With the assumption that all reactions have reached equilibriums, there results a new set of equilibrium equations as given below

$$K_2 = \frac{k_2}{k_{2r}} = \frac{[DAG^-][E]}{[TAG][RO^-]}$$

$$K_4 = \frac{k_4}{k_{4r}} = \frac{[MAG^-][E]}{[DAG][RO^-]}$$

$$K_6 = \frac{k_6}{k_{6r}} = \frac{[G^-][E]}{[MAG][RO^-]} \quad (\text{A-13})$$

Combining equation (A-13) with equation (A-10), the following equilibrium constants are obtained

$$K'_2 = K_2 K_3 = \frac{[DAG][E]}{[TAG][ROH]} = \frac{DAG \cdot E}{TAG \cdot ROH} = \frac{k'_2}{k'_{2r}}$$

$$K'_4 = K_4 K_5 = \frac{[MAG][E]}{[DAG][ROH]} = \frac{MAG \cdot E}{DAG \cdot ROH} = \frac{k'_4}{k'_{4r}}$$

$$K'_6 = K_6 K_7 = \frac{[G][E]}{[MAG][ROH]} = \frac{G \cdot E}{MAG \cdot ROH} = \frac{k'_6}{k'_{6r}} \quad (\text{A-14})$$

This directly results to

$$DAG = K'_2 \frac{1-E}{E} TAG$$

$$MAG = K_4' \frac{1-E}{E} DAG = K_2' K_4' \left(\frac{1-E}{E} \right)^2 TAG$$

$$G = K_6' \frac{1-E}{E} MAG = K_2' K_4' K_6' \left(\frac{1-E}{E} \right)^3 TAG \quad (A-15)$$

Substituting (A-15) into the first balance equation of (A-11) gives

$$TAG = \frac{1}{1 + K_2' \left(\frac{1-E}{E} \right) + K_2' K_4' \left(\frac{1-E}{E} \right)^2 + K_2' K_4' \left(1 + K_6' \frac{1-E}{E} \right)^3} \quad (A-16)$$

Substituting (A-15) and (A-16) into the fourth balance equation of (1-11) yields

$$n = \frac{1}{E} \left\{ 3 - \frac{3 + 2K_2' \left(\frac{1-E}{E} \right) + K_2' K_4' \left(\frac{1-E}{E} \right)^2}{1 + K_2' \left(\frac{1-E}{E} \right) + K_2' K_4' \left(\frac{1-E}{E} \right)^2 + K_2' K_4' K_6' \left(1 + K_6' \frac{1-E}{E} \right)^3} - p \right\} \quad (A-17)$$

Solving equation (A-17), for any E and p (molar ratio of hydroxide (catalyst) to TGA), establishes the amount of alcohol needed for the reaction.

Appendix B: Experimental Data Sheets

B-1 Jatropha Curcas Oil

Experimental data for Jatropha Curcas oil used in this research project is obtained from (Pedavoah, 2010) for RSM analysis and (Mu'azu, *et al.*, 2015) for kinetic modeling. To validate the model data from (Veljkovic', *et al.*, 2006) and (Ude, *et al.*, 2016) is used.

B-1.1. Data for response surface methodology plots.

Table B- 1: Experimental data for biodiesel synthesis using Jatropha Curcas at various conditions (Pedavoah, 2010)

Time (min)	Temperature (°C)	Speed(RPM)	% Yield
60	65	500	74.1
60	65	0	86.11
60	55	0	87.04
45	55	0	87.04
45	65	500	81.79
45	55	500	79.23
45	65	0	83.02
60	55	500	76

B.1.2. Reaction conditions: Kinetic modeling

The concentration time data for pretreated Jatropha Curcas (L.) were adapted from (Mu'azu, *et al.*, 2015) and are given in tables B-3 –B-5. The transesterification of oil was performed under the following experimental conditions:

Table B- 1: Reaction conditions for Jatropha Curcas oil

Reaction time	60 minutes
Catalyst type	Calcium Oxide (CaO)
Catalyst concentration	8% w of oil
Alcohol type	Methanol

Alcohol to oil molar ratio	10:1
Temperature range	55°C
Stirring rate	700rpm

Table B-3: Concentration-time data at T=55°C

	T=55°C					
time(min)	TG	DG	MG	ME	G	ROH
0	7.4	2.6	0	0	0	100
5	4	2.4	2.2	4	1.2	96.2
10	2.8	2.2	1.8	7.8	2.8	92.6
15	1.8	1.8	1.73	12.5	3.1	89.07
20	1.2	1.6	1.72	15	3.2	87.28
25	0.98	1.5	1.71	17.1	3.21	85.5
30	0.9	1.5	1.71	17.2	3.25	85.44
35	0.85	1.5	1.71	17.8	3.25	84.89
40	0.71	1.5	1.7	17.82	3.26	85.01
45	0.2	1.4	1.7	17.85	3.26	85.59
50	0.09	1.4	1.7	18	3.28	85.53
55	0.015	1.4	1.7	18.5	3.28	85.105
60	0.011	1.4	1.7	18.5	3.28	85.109

Table B-4: Concentration time at T=45°C

	T=45°C					
time(min)	TG	DG	MG	ME	G	ROH
0	7.4	2.6	0	0	0	100
5	6	2.2	2.2	5.3	3.2	91.1
10	4.9	2.1	1.8	12.2	4.4	84.6
15	4	1.7	1.63	17.5	5.1	80.07
20	2.9	1.6	1.62	20	5.2	78.68

25	1.9	1.4	1.61	20.9	7	77.19
30	1.8	1.4	1.61	20.9	7.1	77.19
35	1.8	1.4	1.61	21	7.2	76.99
40	1.8	1.4	1.6	20.9	7.1	77.2
45	1.6	1.3	1.6	20	7	78.5
50	1.6	1.3	1.6	21.2	7.2	77.1
55	1.5	1.3	1.6	21.2	7.3	77.1
60	0.98	1.3	1.6	21.2	7.3	77.62

Table B-5: Concentration-time data (mol/L) at T=50°C

		T=50oC			
TG	ME	G	DG	MG	ROH
7.4	0	0	2.6	0	100
5.8	4.8	3	2.4	2.2	91.8
4.1	8.1	3.9	2.2	1.8	89.9
3.2	13	5	1.8	1.63	85.37
2.6	15.1	6	1.6	1.62	83.08
2.6	17	6	1.4	1.61	81.39
2.6	17.1	6	1.4	1.61	81.29
2.4	17.1	6	1.4	1.61	81.49
2.4	17.2	6	1.4	1.6	81.4
1.2	17.8	6	1.3	1.6	82.1
1.2	18	6	1.3	1.6	81.9
0.09	18	6	1.3	1.6	83.01
0.09	18.3	6	1.3	1.6	82.71

B.2 Model validation data

B.2.1 Tobacco seed oil

The experimental data of the transesterification of TSO is adapted from (Veljkovic', *et al.*, 2006).

Table B-6: Reaction conditions for Tobacco seed oil

Reaction time	60 minutes
Catalyst type	Potassium Hydroxide (KOH)
Catalyst concentration	1% w of oil
Alcohol type	Methanol
Alcohol to oil molar ratio	6:1
Temperature	60°C
Stirring rate	400rpm

Table B-7: Concentration-time data at 60°C

	DG	MG	TG	G	ROH	FAME
Time (min)	moles	moles	moles	moles	moles	moles
0	0.02904	0.09504	0.8778	0	6	0.32076
3	0.0924	0.1716	0.462	0.31284	5.68716	0.6336
5	0.10428	0.07128	0.264	0.57684	5.42316	0.8976
10	0.09108	0.0528	0.2376	0.85404	5.14596	1.1748
15	0.0792	0.05016	0.132	0.86724	5.13276	1.188
25	0.08052	0.02376	0.1188	0.88044	5.11956	1.2012
40	0.07788	0	0.0924	0.93324	5.06676	1.254
60	0.066	0	0.06336	0.97284	5.02716	1.2936

B.2.2 Jatropha curcas (homogenous catalysis)

Table B-8: Reaction conditions for Jatropha curcas (Homogeneous)

Reaction time	60 minutes
Catalyst type	Sodium hydroxide (NaOH)
Catalyst concentration	0.6% w of oil
Alcohol type	Methanol
Alcohol to oil molar ratio	6:1
Temperature range	50-60°C
Stirring rate	500rpm

Table B-9: Conversion-time data for Jatropha curcas

Time(min)	X _{tg} (T= 50oC)	X _{tg} (T=60oC)
3	0.894601	0.893541
5	0.899741	0.917915
10	0.909282	0.918732
20	0.911078	0.925726
30	0.917915	0.926465
40	0.91954	0.929349
50	0.93919	0.93919
60	0.959238	0.950213

Appendix C: Simulation Codes

CI. MATLAB CODE FOR RESPONSE SURFACE METHODOLOGY

Jatropha Curcas Oil (Pedavoah, 2010)

%PARAMETER ESTIMATION FOR POLYNOMIAL REGRESSION MODEL FOR
INFLUENCE OF

% TEMP, TIME AND STIRRING RATE ON BIODIESEL YIELD)

Y=[74.1 86.11 87.04 87.04 81.79 79.23 83.02 76];% response Biodiesel Yield (vol%)

T=[65 65 55 55 65 55 65 55];% Factor 1, Temperature (0C)

t=[60 60 60 45 45 45 45 60];% factor 2, reaction time (min)

R=[500 0 0 0 500 500 0 500];% Factor 3, Stirring rate (rpm)

TT=T.*T;% product of the Temperature

tt=t.*t; % product of the reaction time

RR=R.*R;% product of stirring rate

tT=t.*T;% product of Temp and time

TR=T.*R; % product of Temperature and stirring rate, 2nd order interaction

tR=t.*R; %product of time and stirring rate, 2nd order interaction

ttR=t.*t.*R; %product of time and stirring rate, 3rd order interaction

ttT=t.*t.*T; % product of time and temperature, 3rd order interaction

TTt=T.*T.*t;% product of temperature and time, 3rd order interaction

TTR=T.*T.*R;% product of temperature and stirring rate, 3rd order interaction

RRt=R.*R.*t;% product of time and stirring rate, 3rd order

RRT=R.*R.*T;% product of temperature and stirring rate, 3rd order

tRT=t.*R.*T;% product of time, temperature and stirring rate, 3rd order

TTT=T.*T.*T;% product of temperature, 3rd order interaction

ttt=t.*t.*t;% product of time, 3rd order interaction

RRR=R.*R.*R;% product of stirring rate, 3rd order interaction

% 1st order

% PHI=[ones(length(Y'),1)];% Model-0

% PHI=[ones(length(Y'),1) T' t' R']; %Model-1

```

%2nd order
%PHI=[ones(length(Y'),1) T' t' R' TT' tt' RR' tT' TR' tR']; % Model-2
%PHI=[ones(length(Y'),1) T' t' R' tT' TR' tR']; % Model-3
%PHI=[ones(length(Y'),1) T' t' R' TT' tt' RR']; % Model-4

%3rd order
%PHI=[ones(length(Y'),1) T' t' R' TT' tt' RR' ttT' ttR' TTt' TTR' RRt' RRT']; % Model-5
%PHI=[ones(length(Y'),1) T' t' R' TT' tt' RR' TTT' ttt' RRR']; % Model-6
%PHI=[ones(length(Y'),1) T' t' R' tT' tR' TR' ttt' TTT' RRR']; % Model-7
%PHI=[ones(length(Y'),1) T' t' R' TT' tt' RR' tT' tR' TR' ttt' TTT' RRR']; % Model-8
%PHI=[ones(length(Y'),1) T' t' R' TT' tt' RR' tT' tR' TR' ttT' ttR' TTt' TTR' RRt' RRT' ttt'
TTT' RRR']; % Model-9
%PHI=[ones(length(Y'),1) T' t' R' tT' Rt' TR' ttT' ttR' TTt' TTR' RRt' RRT']; % Model-10
%PHI=[ones(length(Y'),1) T' t' R' TT' tt' RR' TRt']; % Model-11
%PHI=[ones(length(Y'),1) T' t' R' TT' tt' RR' tT' tR' TR' ttt' TTT' RRR' TRt']; % Model-12

th=inv(PHI*PHI)*PHI*Y'
estimated_error=Y'-PHI*th;
Y2=Y'-estimated_error
B=inv(PHI*PHI)*PHI*(estimated_error);
C=mean(B);
Mean_error =mean(estimated_error)
variance_residual=var(estimated_error)
N=length(T);
P=length(th);
Mean=[th(1) th(2) th(3) th(4) th(5) th(6) th(7) th(8) th(9) th(10)]; %th(11) th(12) th(13)];%
th(14)];% th(15)]; %th(16) th(17) th(18) th(19) th(20) th(21)];
covarianceth = variance_residual*(N-1)/(N-P)*inv(PHI*PHI);

```

C2. Code for generating Response Surface Plots with equation of best fit

```
Xp=[55:0.91:65;0:45.5:500 ;15:4.1:60]';
t=60;
for i=1:11, for j=1:11, z= 99.0887-0.1072*Xp(i,1)-0.1305*t-0.016*Xp(j,2);Z(i,j)=z;end;end;

mesh(Xp(:,1),Xp(:,2),Z')
xlabel('Temperature (oC)')
ylabel('Stirring rate (rpm)')
zlabel('Yield (vol%)')

contour(Xp(:,1),Xp(:,2),Z')
xlabel('Temperature (oC)')
ylabel('Stirring rate (rpm)')
```

C3. SCILAB Code for solving six ordinary rate equations

// batch reactor

```
clear;clc();lines(0);
f=gda();fontsize=3;
f.title.font_size=fontsize+1;
f.x_label.font_size=fontsize+2;
f.y_label.font_size=fontsize+2;
f.z_label.font_size=fontsize+2;
f.font_size=fontsize;
f.thickness=2;

// data
names=['TG' 'DG' 'MG' 'G' 'FAME' 'ROH'];

C0(1)=7.4;

C0= [7.4 2.6 0 0 0 100]';
```



```

k1=0.0006
k2=0.1
k3=0.21703372
k4=0.008366371
k5=0.1
k6=0.530436626

```

```

function f=batch(t, c)

```

```

    f(1)=-k1*c(1)*c(6)+ k2*c(2)*c(5);

```

```

    f(2)=k1*c(1)*c(6)-k2*c(2)*c(5)-k3*c(2)*c(6)+k4*c(3)*c(5);

```

```

    f(3)=k3*c(2)*c(6)-k4*c(3)*c(5)+k6*c(4)*c(5)-k5*c(3)*c(6);

```

```

    f(4)=k5*c(3)*c(6)-k6*c(4)*c(5);

```

```

    f(5)=k1*c(1)*c(6)-k2*c(2)*c(5)+k3*c(2)*c(6)-k4*c(3)*c(5)+k5*c(3)*c(6)-
k6*c(4)*c(5);

```

```

    f(6)=-f(5);

```

```

endfunction

```

```

t=[0 5 10 15 20 25 30 35 40 45 50 55 60]';

```

```

TG=[7.4 4 2.8 1.8 1.2 0.98 0.9 0.85 0.71 0.2 0.09 0.015 0.011]';

```

```

DG=[2.6 2.4 2.2 1.8 1.6 1.5 1.5 1.5 1.5 1.4 1.4 1.4 1.4]';

```

```

MG=[0 2.2 1.8 1.73 1.72 1.71 1.71 1.71 1.7 1.7 1.7 1.7]';

```

```

G=[0 1.2 2.8 3.1 3.2 3.21 3.25 3.25 3.26 3.26 3.28 3.28 3.28]';

```

```

FAME=[0 4 7.8 12.5 15 17.1 17.2 17.8 17.82 17.85 18 18.5 18.5]';

```

```

ROH=[100 96.2 92.6 89.07 87.28 85.5 85.44 84.89 85.01 85.59 85.53 85.105 85.109]'

```

```

// calculations

```

```

t0=0; t1=60

```

```

t=linspace(t0,t1,101)

```

```

C=ode(C0,t0, batch)

```

```

//plot]

```

```

scf(1);clf(1);
title('Concentration vs time plot at k = 1')
plot(t,C(1,:), 'black')
plot(t,C(2,:), 'red')
plot(t,C(3,:), 'magenta')
//plot(t,C(4,:), 'green')
plot(t,C(5,:), 'blue')
//plot(t,C(6,:), 'yellow')
t=[0 5 10 15 20 25 30 35 40 45 50 55 60]
plot(t,FAME, 'blue')
plot(t,TG, 'black')
plot(t,DG, 'red')
plot(t,MG, 'magenta')
//plot(t,G, 'green')
//legend('exp FAME'
legend('TG','DG','MG','G','sim FAME','exp FAME')
xtitle(',$Time \; \; [min]$', '$C_i \; \; [mol.L^{-1}]$')

scf(2);clf(2);

plot(t,FAME, '-o-blue')
t0=0; t1=60
t=linspace(t0,t1,101)
plot(t,C(5,:), 'blue')
legend('exp FAME','sim FAME')
xtitle(',$Time \; \; [min]$', '$Concentration \; \; [mol.L^{-1}]$')
ObjectFunc= sum(FAME)
ObjFunc=sum(C(5,:))
SSqrt=(ObjectFunc-ObjFunc)^2

// plot conversion

//scf(6);clf(6);
//title('Conversion vs time plot at k = 1')

```

```

//XA=(C0(1)-C(1,:))/C0(1)
//plot(t,XA)
//xtitle('','$Time \;[min]$', '$Conversion $')

//plot experimental data
scf(3);clf(3);
t=[0 5 10 15 20 25 30 35 40 45 50 55 60]';
TG=[7.4 4 2.8 1.8 1.2 0.98 0.9 0.85 0.71 0.2 0.09 0.015 0.011]';
DG=[2.6 2.4 2.2 1.8 1.6 1.5 1.5 1.5 1.5 1.4 1.4 1.4 1.4]';
MG=[0 2.2 1.8 1.73 1.72 1.71 1.71 1.71 1.7 1.7 1.7 1.7 1.7]';
G=[0 1.2 2.8 3.1 3.2 3.21 3.25 3.25 3.26 3.26 3.28 3.28 3.28]';
FAME=[0 4 7.8 12.5 15 17.1 17.2 17.8 17.82 17.85 18 18.5 18.5]';
ROH=[100 96.2 92.6 89.07 87.28 85.5 85.44 84.89 85.01 85.59 85.53 85.105 85.109]';
plot(t,FAME,'blue')
plot(t,TG,'black')
plot(t,DG,'red')
plot(t,MG,'magenta')
//plot(t,G,'green')
//plot(t,ROH,'yellow')
//plot(t,C(5,:),'blue')
legend('exp FAME','TG','DG','MG','G')
xtitle('','$Time \;[min]$', '$Concentration \;[mol.L^{-1}]$')

//plot Yield
//Y=(C)/(C0(1)+C0(2))
//scf(3);clf(4);
//plot(t,Y(3,:),t,Y(4,:))
//xtitle('$Yield\;Vs\;time(min)\;','$t(min)$','$Y_j$')
//h1=legend(['C' 'D'],a=2)
//drawnow

//Varying k value code

```

```

scf(10);clf(10);

//for i = 0.01:0.1:1

// k = ones(1,6).*i;
// calculations
//t0=0; t1=60
//t=linspace(t0,t1,101)
//C=ode(C0, t0,t,batch)

//plot]
//title('Concentration vs time plot at k '+k)

//title('Conversion vs time plot at varying ks')
//XA=(C0(1)-C(1,:))/C0(1)
//t0=0; t1=60
//t=linspace(t0,t1,101)
//plot(t,XA)
//xtitle('','$Time \; \; [min]$', '$Conversion \; TG$')

//end
scf(10);clf(10);
title('Conversion vs time plot at varying ks')
XA=(C0(1)-TG)/C0(1)
t=[0 5 10 15 20 25 30 35 40 45 50 55 60]'

plot(t,XA)
xtitle('','$Time \; \; [min]$', '$Conversion \; TG$')

```